Geothermics 136 (2026) 103604

Contents lists available at ScienceDirect

Geothermics

journal homepage: www.elsevier.com/locate/geothermics

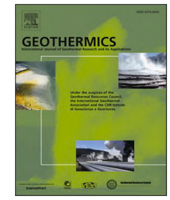

Three-dimensional lithospheric-scale thermal model as supporting tool for new exploration campaigns for geothermal resources: Insights from the Calabria region (Southern Italy)

G. Vespasiano [a,b,*], G. Floridia [c,**], M. Giuffrida [c], M. Viccaro [c,d], A. Bloise [a,*], R. De Rosa [a], M. Cacace [e], I. Fuoco [a], M.F. La Russa [a], F. Muto [a], R. Dominici [a,b], L. Russo [a,f], M. Cipriani [a], A. Guido [a], G. Maruca [a], C. Apollaro [a]

[a] Dipartimento di Biologia, Ecologia e Scienze della Terra, Università della Calabria, Via P. Bucci, cubo 15b, Rende, Cosenza, Italy
[b] E3 (Earth, Environment, Engineering) Soc. Coop. and Spin-Off of University of Calabria, Via Ponte Bucci, Cubo 15B, 87036 Rende, Italy
[c] Università degli Studi di Catania, Dipartimento di Scienze Biologiche Geologiche e Ambientali, Corso Italia 57, Catania, Italy
[d] Istituto Nazionale di Geofisica e Vulcanologia – Sezione di Catania, Osservatorio Etneo, Piazza Roma 2, Catania, Italy
[e] Helmholtz Centre Potsdam GFZ German Research Centre for Geosciences, Telegrafenberg, Potsdam, Germany
[f] Istituto per la Tecnologia delle Membrane (ITM-CNR), Rende (CS), Italy

ARTICLE INFO

Keywords:
Lithospheric model
Thermal modelling
Geothermal exploration
Calabria Region

ABSTRACT

This study presents the first lithosphere-scale, steady-state 3D thermal model of the Calabria region (Southern Italy), developed to support the geothermal resource assessment and exploration. By integrating geological, geophysical, and thermal datasets, a high-resolution 3D geological model was built and used as a structural framework for finite-element thermal simulations. The simulations incorporated spatially variable thermal conductivity, radiogenic heat production, and a range of basal heat flux values applied at the crust-mantle (Moho) interface. Five thermal scenarios were tested and calibrated against 254 measured temperature data points from exploration wells. The results reveal pronounced lateral thermal heterogeneity, with temperatures exceeding 90 °C at 3 km depth beneath the Ionian basins, driven by the local crustal structure, sedimentary blanketing, and Moho geometry. While the model delineates zones suitable for low-to-medium enthalpy geothermal exploitation (1-3 km), deeper high-enthalpy targets remain less constrained and deserve further investigation. This study establishes a geologically consistent framework that enhances the understanding of the regional thermal regime and serves as a strategic tool for guiding future geothermal exploration in Calabria.

1. Introduction

Over the past century, energy production has predominantly relied on fossil fuels. However, the increasing awareness of their environmental and health consequences, combined with their limited capacity to satisfy the rising energy needs, has led to a transition toward sustainable alternatives (Moya et al., 2018). Among these, geothermal energy stands out for its wide range of applications, low emissions, and adaptability to various geological settings (Rybach and Mongillo, 2006; Zhu et al., 2015). Its effective exploitation requires a detailed understanding of regional geological and tectonic settings, supported by direct investigations such as deep drilling (Alçiçek et al., 2019; Hou et al., 2018). Nevertheless, the use of thermal modeling as a preliminary step for exploration is crucial as it enhances the targeting of promising areas and optimizes exploration strategies (Floridia et al., 2022; Marini et al., 2025). Advances in computational techniques have facilitated the development of local thermal models, which augment conventional methods by improving the understanding of subsurface temperature patterns (Giuffrida et al., 2025).

The focus of this study is the Calabria region in southern Italy, a geodynamically complex area with considerable, but yet unexplored geothermal resources. This research aims to reconstruct the steady-state 3D thermal fields of Calabria through a multidisciplinary workflow. The construction of a high-resolution 3D geological model, combined with

* Corresponding authors at: Dipartimento di Biologia, Ecologia e Scienze della Terra, Università della Calabria, Via P. Bucci, cubo 15b, Rende, Cosenza, Italy.
** Corresponding author at: Università degli Studi di Catania, Dipartimento di Scienze Biologiche Geologiche e Ambientali, Corso Italia 57, Catania, Italy.
E-mail addresses: giovanni.vespasiano@unical.it (G. Vespasiano), giovanni.floridia@phd.unict.it (G. Floridia), andrea.bloise@unical.it (A. Bloise).

https://doi.org/10.1016/j.geothermics.2026.103604
Received 7 October 2025; Received in revised form 22 December 2025; Accepted 13 January 2026
Available online 20 January 2026
0375-6505/

the simulation of the steady-state thermal field, was carried out by integrating geological, geophysical, and thermal datasets using specialized computational tools. Among the various parameters, thermal conductivity, radiogenic heat production, and boundary conditions, such as crust-mantle heat flux, play a key role in the modelling procedure. At the end of the simulation processes, multiple models were generated and subsequently tested to ensure optimal correlation with in-situ temperature measurements. These thermal models and temperature-depth maps, constructed for different stratigraphic levels, allowed the quantification of the total heat budget, the assessment of low-to-high geothermal resources, and the identification of the most suitable sites for potential geothermal development. Ultimately, this study is aimed at facilitating the sustainable energy transition and enhancing the regional energy independence by establishing a comprehensive framework for geothermal exploitation, grounded in a detailed characterization of subsurface thermal and geological properties.

2. Geological and geodynamic framework

The Calabria-Peloritani Orogen (CPO) represents an arcuate ribbon-like segment of the peri-Mediterranean orogenic Alpine nappe system encompassing the Calabria region and the eastern sector of Sicily (Cirrincione et al., 2015 and references therein). The CPO is positioned between the Pollino Fault Zone (PFZ – Fig. 1), to the north, and the Taormina Line to the south (TL – Fig. 1), acting as a structural link between the Apennine thrust-and-fold belts of southern Italy and the Maghrebian chain in Sicily (Bonardi et al., 1980; Tortorici, 1982; Carminati et al., 2010). The CPO comprises various basement nappes and ophiolite-bearing tectonic units that are remnants of the Cretaceous-Paleogene Eo-Alpine orogeny and were involved in the Neogene formation of the Apennine orogenic belt (Rossetti et al., 2001; Cifelli et al., 2008; Carminati et al., 2010; Villamizar Escalante et al., 2025). Geologically and morphologically, the CPO can be subdivided into two distinct sectors, separated by the Catanzaro line (CL) (Fig. 1): a northern sector, which includes the Sila Massif and the Coastal Chain, and a southern sector, consisting of the Serre and Aspromonte massifs along with the Peloritani Mountains in Sicily. This subdivision, which has been subject to ongoing re-evaluation (Tortorici, 1982; Cirrincione and Pezzino, 1991; Pezzino et al., 2008; Cirrincione et al., 2008, 2012), remains geologically significant as it separates two sectors with notably distinct geological histories. The northern sector is represented by a Europe-verging nappe-like structure of Eocene age (Dietrich, 1988; Cello et al., 1996) that overlapped during the early-Miocene onto the African continental margin. This sector shows exclusive Africa verging transport since the early Oligocene and up to Miocene, with associated deposition of a huge conglomerate and arenaceous-pelitic succession known as Capo d'Orlando Formation (Cirrincione, 1996; Atzori et al., 2000; Cavazza and Ingersoll, 2005). The nappe structures of Sila and Coastal Chain cover the entire northern sector of the orogen (Fig. 1). They are separated by the Crati valley, a N-S trending graben ascribed to the Pliocene-Pleistocene (Tortorici et al., 1995; Tansi et al., 2007, 2016, 2024). These structures consist of three main tectono-stratigraphic complexes, each formed by distinct tectono-metamorphic units (Amodio-Morelli et al., 1976; Piluso et al., 2000; Scandone, 1982): (i) the basal "Apennine Complex" made up of partly metamorphosed

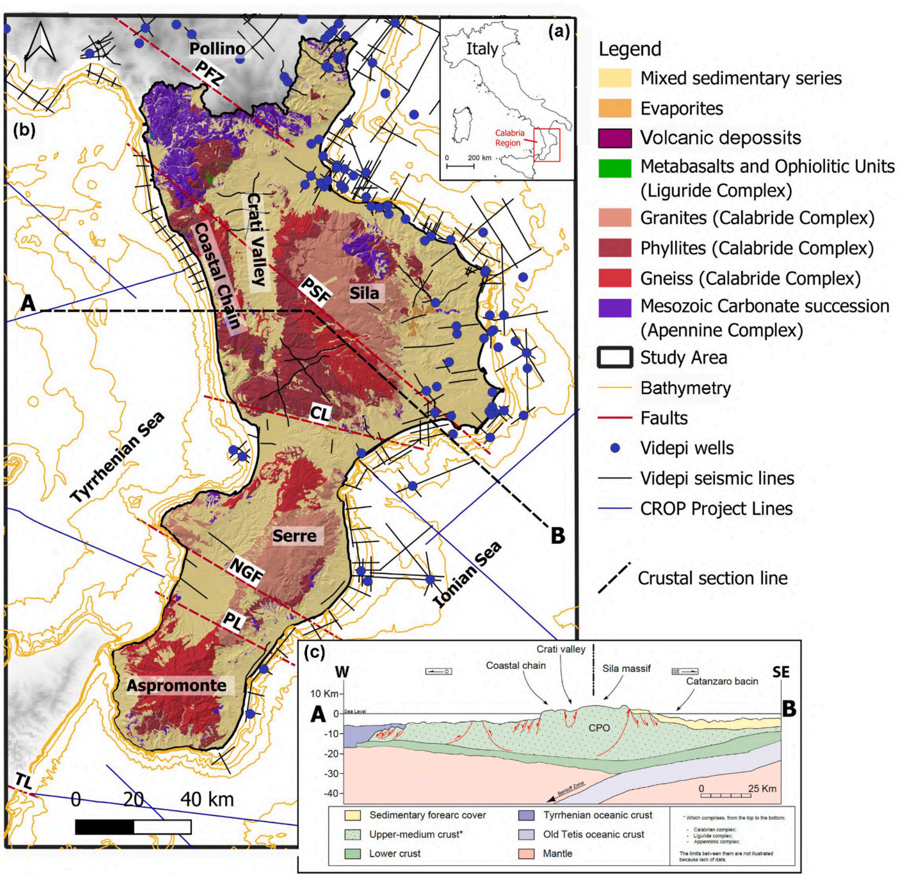

Fig. 1. a) Location of the study area (Calabria Region – South Italy). b) Simplified geological map of the Calabria Region. The figure shows all data acquired for the final elaboration: VIDEPI project (seismic line and wells); CROP project (Scrocca, 2003 - seismic line); DEM of Calabria Region (25m*25m); Bathymetric map (from the EMODnet Digital Terrain Model - Thierry et al., 2019); GEOTHOPICA database; Moho map (Barberi et al., 2004; Calò et al., 2012; Di Stefano and Ciaccio, 2014; Grad et al., 2009). c) Schematic crustal section (modified after Van Djik et al., 2000). **PSF:** Petilia-Sosti Fault; **PZF:** Pollino Fault Zone, **CL:** Catanzaro line, **NGF:** Nicotera Gioiosa Fault, **TL:** Taormina Line, **PL:** Palmi Line.

Mesozoic carbonate succession (Ietto and Barillaro, 1993; Perrone, 1996; Ietto and Ietto, 1998; Iannace et al., 2007); (ii) the intermediate Liguride Complex consists of oceanic-derived units, interpreted as remnants of the Tethys Ocean (Guerrera et al., 1993; Cello et al., 1996; Tortorici et al., 2009); (iii) the upper Calabride Complex representing an uninterrupted continental crust section developed during the late Variscan orogeny (Thomson, 1994; Brandt and Shenk, 2020). The western and eastern margins of Calabria are covered by Neogene-Quaternary clastic deposits that successively infill the Peri-tyrrhenian and Periionian basins (Van Dijk et al., 2000; Mattei et al., 2002; Muto and Perri, 2002; Zecchin et al., 2020, and references therein). Within the Neogene stratigraphic record of these basins, Messinian evaporitic units (resedimented gypsum, microbial limestones, and basin-centred halite deposits; Guido et al., 2007; Birgel et al., 2014; Cipriani et al., 2024, 2026; Dominici et al., 2025) may occur and act as mechanically weak horizons, influencing both basin architecture and fault kinematics.

The southern sector of the Calabria region is characterized by the Serre Massif, the Capo Vaticano Promontory (both considered to represent a continuous continental crustal section closely associated with that of the Sila and Catena Costiera areas) and the Aspromonte Massif (Fig. 1). Unlike the northern sector, no elements attributable to the Liguride or Apennine Units complexes are present at the base of these massifs (Cirrincione et al., 2015). The Aspromonte Massif occupies the southern end of Calabria, bordered to the north by the crustal-scale strike-slip fault system known as Palmi Line (PL - Ortolano et al., 2013; Tripodi et al., 2018, 2022). It is a south-east verging nappe edifice (Ortolano et al., 2015), where the two uppermost tectonic slices are constituted by two middle-upper crust derived units (the upper Stilo Unit and the lower Aspromonte Unit), both characterised by a multi-stage Variscan metamorphism, locally involving only the deeper one during the latest stages of the Alpine metamorphic cycle (Bonardi et al., 1984a, 1984b, 1992; Graessner and Schenk, 1999; Platt and Compagnoni, 1990; Ortolano et al., 2005; Pezzino et al., 2008). The deepest tectonic unit, separated by the intermediate Aspromonte Unit, shows a thick mylonitic horizon and is composed of medium-grade metapelites, exclusively registered a complete Alpine metamorphic cycle (Pezzino et al., 1990, 2008; Ortolano et al., 2005; Cirrincione et al., 2008; Fazio et al., 2008).

3. Geothermal potential of the Calabria region

The Calabria region is one of the most interesting areas in the Mediterranean in terms of geothermal potential. Despite well-known socio-economic challenges, Calabria claims significant geothermal potential, highlighted by numerous thermal springs scattered across the region. The intricate geological and structural framework, coupled with active tectonics, creates favourable conditions for non-magmatic convection-dominated geothermal systems, either fault-controlled or fault-leakage-controlled, according to the catalogue of Moeck (2014). Thermal springs in Calabria have been the subject of various investigations, with both regional and site-specific approaches (e.g., Bencini and Ciracò, 1982; Gurrieri et al., 1984; Duchi et al., 1991; Calcara and Quattrocchi, 1993; Italiano et al., 2010). More recently, site-specific approaches were adopted in the studies of Apollaro et al., (2012, 2016, 2019, 2020, 2025) and Vespasiano et al., (2014, 2015a, 2015b, 2015c, 2016, 2023). These works showed that the main geothermal reservoirs in northern Calabria are hosted in the deep Mesozoic carbonate units, which are sporadically exposed in tectonic windows, allowing the discharge of thermal waters. In contrast, southern Calabria's geothermal reservoirs are predominantly hosted in basal crystalline-metamorphic units. These geochemical studies identified the origin of thermal fluids, the processes during their ascent and helped to establish the conceptual model of the Calabria thermal systems. However, these results constitute only an initial step in assessing the region's geothermal potential, focusing on localized areas. The subsequent crucial step involves evaluating temperature and heat flux distribution, encompassing both conductive and advective heat transfer.

Beyond characterizing localized thermal springs, other projects aimed to define the medium- to low-temperature geothermal potential across the entire region. Among these, the most important was the VIGOR project (Evaluation of the geothermal potential of the convergence regions, Campania-Puglia-Calabria-Sicily, Galgaro et al., 2012; Iovine et al., 2012), which proved to be useful in providing analytical information to start geothermal prospecting activities and to increase the share of energy consumed from renewable sources, as well as to improve energy efficiency and to promote local development activities.

The geothermal resources of the Calabria region are still largely geologically undefined and require adequate assessment using innovative exploration strategies, such as integrative thermal modelling assisted by geological constraints. In this context, geochemical data and wells drilled during the hydrocarbon exploration campaigns in the 50s and 60s, covering localised portions of the Calabrian territory and providing well-log data (thermometric, sonic, and gamma-ray data), are helpful for studying regional geothermal conditions. From a general point of view, few studies consider and develop numerical models to evaluate the heat exchange in the subsoil. In Italy, a few studies have been carried out to map the geothermal potential of regions based on 3D analytical modelling approaches (Basilici et al., 2019; Basilici et al., 2020; Santini et al., 2020; Santini et al., 2021), revealing that understanding the 3D temperature distribution on a regional scale is an essential step to investigate the geothermal potential and stimulate interest in its exploitation.

4. Methodologies

4.1. 3D geological modelling approach

Accurately assessing the thermal regime of the Calabria region hinges on a detailed understanding of its crustal framework, particularly its lithology and associated physical properties. Integrating extensive datasets is a powerful strategy for evaluating geothermal resources, which directly improves the efficiency and precision of subsequent numerical modelling.

A key gap in existing research is the absence of comprehensive regional studies that synthesize the limited available data on Calabria's subsurface complexity and its impact on the thermal field. To fill this void, we began with a regional 3D geological model and integrated all pertinent geological and geophysical data (Fig. 1) to create an initial model geometry (Fig. 2). This dataset includes interpretations of seismic lines (from a variety of sources, including Cello et al., 1981; Cristofolini et al., 1985, and others) and data from hydrocarbon exploration wells (from the VIDEPI and GEOTHOPICA projects and Trumpy et al., 2017).

To establish the model's core geometry, we incorporated available data on the major layers (Fig. 3) and defined the boundaries between lithospheric units. These boundaries were specifically drawn to delineate bodies with homogeneous physical properties by capturing first-order variations in density. Given the low data resolution, we made the simplifying assumption of assigning a single, homogeneous physical property to each 3D layer. Each surface was defined using convergent interpolation algorithms in the PETREL software (©Schlumberger). While we acknowledge the inherent geological heterogeneity of each layer, this simplification was deemed acceptable given the constraints of the available data and the large-scale nature of the study area. Table 1 lists the prevailing lithologies for all the geological model units and their variability in density (g/cm^3).

The first stage involved defining the thicknesses of the units through systematic data analysis and the reconstruction of reference surfaces. All maps proposed in this study were obtained using a geostatistical method, widely employed in geological science, to obtain an unbiased estimate of regionalised variables. The Ordinary Kriging (OK) method minimises the estimation variance (Lewicki et al., 2005) but requires

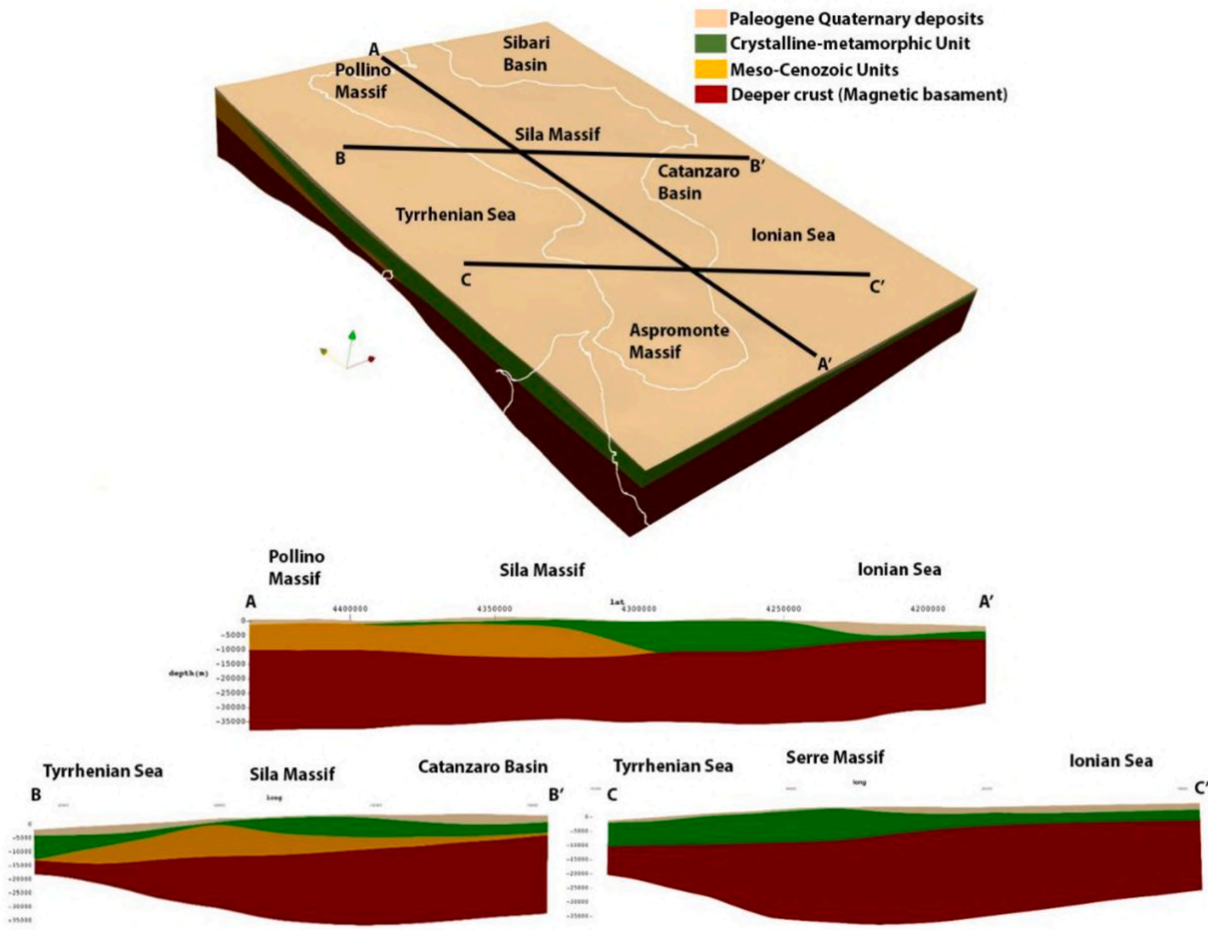

Fig. 2. Regional 3D geological model. Simplified lithological blocks (shown in legend) were generated using MeshIt.

certain assumptions to be applied, such as an unknown constant mean (Webster and Oliver, 2007). OK relies on the dataset semivariance analysis and on the comparison between an experimental semivariogram and theoretical ones (Han and Suh, 2024; Apollaro et al., 2025). The unknown values $Z_{(x0)}$ are calculated by the following OK Eq. (Saito et al., 2005):

$$Z_{(x0)} = \sum_{i=1}^{n} Z_{(xi)} * \lambda_{(i)}$$

Where $Z_{(xi)}$ is the measured/observed value at the location xi, while λ is the weight relative to the residual value of $Z_{(xi)}$.

The upper boundary of the model was defined using two key datasets: the Calabrian Region Digital Terrain Model (DTM) at a 20 m x 20 m resolution and bathymetric data from the EMODnet Digital Terrain Model for European marine areas (Thierry et al., 2019). These datasets form the model's uppermost surface (Fig. 3a, Table 1S).

Within this regional framework, the Paleogene-Quaternary deposits and the Crystalline-Metamorphic Unit are represented as isolated volumes (Figs. 2, 3b, and 3c, Tables 2S and 3S). Specifically, the Oligo-Pleistocene deposits show a significant variation in thickness, ranging from just a few meters near the major massifs (Sila, Pollino, Aspromonte, Serre, Coastal Chain) to approximately 6 km below sea level (b.s.l.) in the main offshore basins (eastern Sibari plain, Locride area, and western Tyrrhenian coastline).

The crystalline-metamorphic unit exhibits a regional thickness that increases southward. In the northern part of the region, it reaches thicknesses of up to 3-4 km b.s.l. near the Sila and Coastal Chain massifs. Conversely, along the northern boundary, where the underlying carbonate units are closer to the surface, the unit is at its thinnest (Fig. 3c). In the southern portion, an assumed thickness of up to 13 km b.s.l. was used due to the absence of deep carbonate units.

The depths of the crystalline basement and the thickness of the Mesozoic carbonates were constrained using interpretations from Trumpy et al. (2016, 2017) and Cassano et al. (1986). The latter introduced the term “magnetic basement” to describe a theoretical surface below which sedimentary successions are no longer present. The magnetic basement is deepest in the northern sector (up to 13 km b.s.l.) and shallower in the southern portion, sometimes falling below 10 km (Fig. 3d, Table 4S). The intersection of the metamorphic crystalline units' base with the magnetic basement enabled the reconstruction of the Mesozoic carbonate domain, which attains a maximum thickness of 12 km b.s.l. in the north and diminishes toward the south.

Finally, to constrain the base of the crust, we reconstructed the Moho depth using data from various studies (Maesano et al., 2017; Barberi et al., 2004, and others). As shown in Fig. 3e (Table 5S), the Moho depth varies from east to west. A deep Moho interface, between 36 and 38 km, characterizes the central CPO, a feature closely linked to the subduction slab setting. The shallowest Moho depths are found in the Tyrrhenian and Ionian domains, with a total crustal thickness of less than 24 km and 30 km b.s.l., respectively.

The final 3D reconstruction was developed using the open-source software MeshIt, which allows generating high-quality tetrahedral meshes for the later simulation stage, (https://www.gfz.de/en/section/subsurface-process-modelling/infrastructure/meshitc), with a lateral resolution of 5 km. The resulting model is composed of five distinct layers from top to bottom, representing significant stratigraphic and

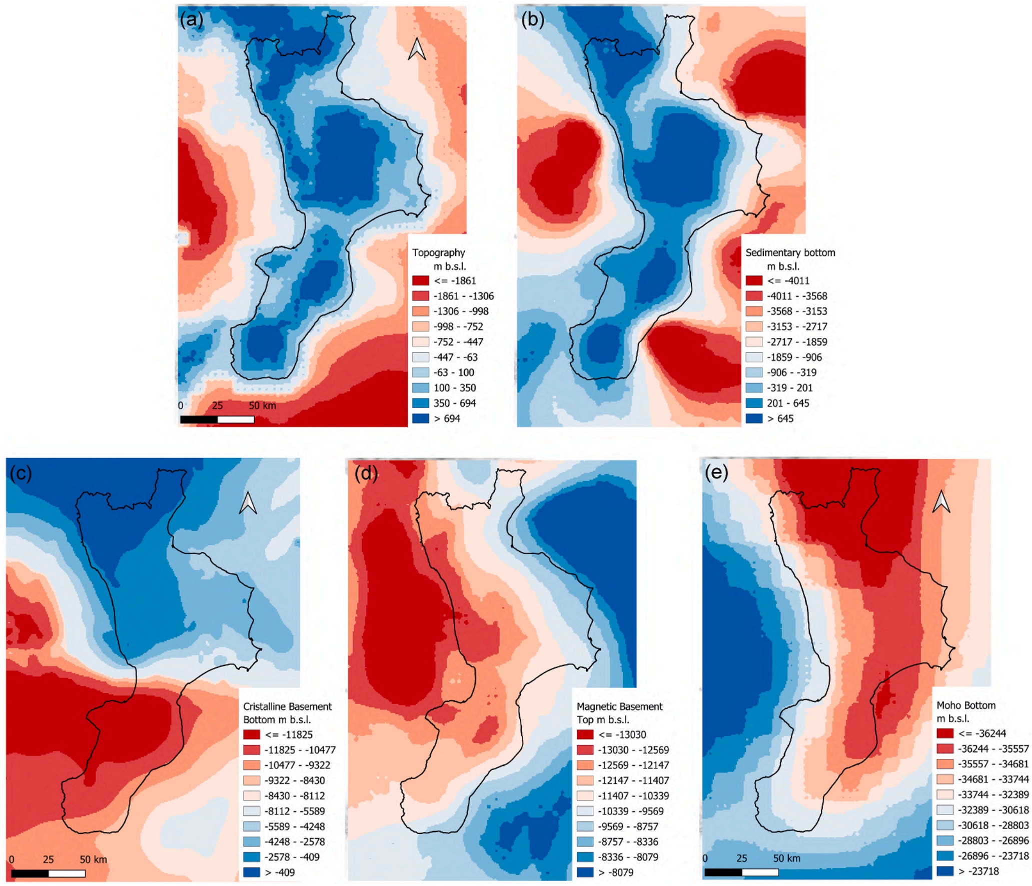

Fig. 3. Depth-elaborated maps of the lithological layers considered for the 3D geological model: (a) Upper boundary of the model represented by topography (topography + bathymetry); (b) bottom of the Paleogene-Quaternary deposits; (c) bottom of the Crystalline Basement; (d) top of the magnetic basement (e) Depth of the mantle/crust boundary (Moho). The depth values for each point of the 5 km resolution grid are shown in the supplementary material.

lithological variations: (1) Paleogene-Quaternary deformed deposits, (2) Crystalline Basement Rocks, (3) Meso-Cenozoic Carbonates, (4) the magnetic basement (as defined by Trumpy et al., 2017), and (5) the Lithospheric mantle. Detailed depth maps of each unit within the 3D model are presented in Fig. 3.

4.2. Thermal modelling and dataset

The developed 3D geological model was used as input for the open-source code GOLEM (Cacace and Jacquey, 2017) to simulate the steady-state conductive thermal field within a structurally complex geological context. GOLEM enables high-resolution thermal simulations by accounting for spatial variations in rock properties, such as thermal conductivity and radiogenic heat production, and by applying geologically consistent boundary conditions, including surface temperature constraints and variable basal heat flux at the crust-mantle interface. The software is specifically designed to model coupled thermal, hydraulic, mechanical, and non-reactive chemical processes. It is implemented within the MOOSE (Multiphysics Object-Oriented Simulation Environment) framework developed by the Idaho National Laboratory. GOLEM utilizes advanced nonlinear solution strategies, such as the classical Newton–Raphson method and the Jacobian-free inexact Newton–Krylov approach, to solve the governing equations describing groundwater flow, heat and mass transport, and rock deformation. Assuming that steady-state conduction is the primary mode of heat transport, the governing equation solved is:

$$\nabla\cdot(\lambda\nabla T) - H = 0$$

where λ denotes the thermal conductivity of the porous medium (in W/m·K), calculated as a volumetric average between the solid matrix and pore spaces, T is the temperature (in Kelvin), and H is the radiogenic heat production term (in W/m^3), treated as an internal heat source.

The geometry and thermal properties of each lithological unit were discretized within a Finite Element Model (FEM), implemented in C++ to enable the numerical simulation. The horizontal resolution of the FEM matches that of the geological model (5 km), while the vertical resolution was refined to maintain an element aspect ratio close to unity. This was achieved by subdividing each geological unit into several finite element layers.

The following boundary conditions were applied to solve for the temperature distribution numerically. All lateral boundaries were assumed to be impermeable to heat flow, and a spatially variable surface temperature (Dirichlet condition) was imposed at the model's top boundary, accounting for topography and bathymetry. This surface temperature distribution was derived by interpolating the annual mean temperature values from the dataset of Brunetti et al. (2014). The lower boundary condition was imposed by estimating the thermal input from the underlying mantle in the regional geological context.

The geological framework, thermal properties assigned to each lithological unit, and defined boundary conditions provided the basis for computing the regional-scale thermal field across Calabria. This modelling effort led to the development of the first lithosphere-scale 3D thermal model of the entire region, aimed at quantifying its thermal structure. Model outcomes were evaluated by varying the lower boundary condition, with a series of simulations conducted to assess the sensitivity of the results to variations in thermal properties. The best-fitting scenarios were compared against available shallow temperature measurements. Due to the absence of direct measurements of

Table 1
Thermal modelling parameters used for the workflow. Values in parentheses ( ) and in brackets [ ] are taken from the corresponding references, reported in parentheses ( ) and in brackets [ ], respectively.

Layer	Dominant lithology	Density reference model (g/cm^3)	Ref.	Thermal conductivity (W/mK)	Ref.	Radiogenic production (mW/m^3)	Ref.	Heat flux (mW/m^2)	Ref.
Paleogene Quaternary deposits	Evaporites and sedimentary	2.02 (2.2 - 2.35) [2.3 - 2.35]	VIDEPI project* (Pepe et al. 2010) [Akimbekova et al. 2023]	1.5-3.0	Di Sipio et al., 2013	0.68 (0.4 - 1.1)	Caracausi et al., 2005; (Vilà et al., 2010)		
Crystalline-metamorphic Unit	Metamorphic and Igneous Rocks	2.78 - 2.9 - (2.69) [2.76 - 2.86]	Punturo et al., 2005; Sgroi et al., 2012; (Pepe et al. 2010) [Akimbekova et al. 2023]	1.9-2.9	Cataldi et al., 1995; Di Sipio et al., 2013; Trumpy and Manzella, 2017	0.68 (0.23 - 2.8)	Vilà et al., 2010		
Meso-Cenozoic Units	Mesozoic Carbonates and evaporites	2.4	VIDEPI project*	2.5-3.9	Montanari et al., 2017; Trumpy and Manzella, 2017	0.5 - 1	Caracausi et al., 2005; Vilà et al., 2010		
Deeper crust (Magnetic Basement)	Granodiorite	2.85 (2.92 - 2.84)	Pepe et al. 2010	2.7-3.5	Clauser and Huenges, 1995; Vilà et al., 2010	0.1 - 1	Vilà et al., 2010; Waples, 2001		
Lithospheric mantle	Peridotite	(3.273 - 3.361) (Plagioclase phase 3.28 - Spinel 3.37) [3.2]	Range from (Fichtner et al., 2018; Kumar, 2022) (Pepe et al. 2010) [Akimbekova et al. 2023]	4	Stacey, 2007	0.03 - 0.016	Vilà et al., 2010		
Moho_min								20	Jaupart et al., 2007
Moho_mean								40	Jaupart et al., 2007
Moho_max								60	Jaupart et al., 2007

* data from the Gardner's relation (Gardner et al., 1974) applied to seismic velocity ViDEPI dataset.

temperature or heat flux at the Moho, a sensitivity analysis was carried out by running models with different heat flux values at the lower boundary, ranging from 20 to 60 mW/m^2, in accordance with global estimates reported by Jaupart (2007). The thermal property values used (Table 1) were determined through a combination of outcrop analyses, hydrocarbon exploration well log interpretations, and laboratory experiments reported in recent literature (e.g., Abate et al., 2014; Galgaro et al., 2012; Gola et al., 2013; Di Sipio et al., 2013, 2014).

For each heat flux scenario, adjustments were made to the thermal properties of each lithological layer. Five modelling scenarios were defined as follows: a) **S1**: Minimum thermal property values proposed in the literature with Moho heat flux set to 20, 40, and 60 mW/m^2 (considering the minimum, maximum and average values proposed in the literature - Jaupart, 2007); b) **S2**: Maximum thermal property values with the same flux range; c) **S3**: Mean thermal property values for the flux range; d) **S4**: Maximum thermal properties applied to the Mesozoic Units only, with variable Moho heat flux; e) **S5**: Maximum thermal properties applied to the Crystalline Units only, with variable Moho heat flux. Radiogenic heat production was assumed constant for each unit, using average values and considering its relatively minor influence on the overall thermal regime. The geological heterogeneity of the Calabrian region results in substantial spatial variability in thermal properties, particularly thermal conductivity (as detailed in Table 1). Given the lack of data indicating preferential heat-conduction directions at the regional modelling scale, thermal conductivity was assumed isotropic. Its potential variation with depth or temperature was also neglected. Each lithological unit was assigned constant, effective thermal parameters based on the dominant rock types derived from previous geological studies. This simplification reflects the inherent complexity of Calabrian lithostratigraphy, which cannot be fully resolved at the regional scale.

5. Results and Discussions

5.1. Regional thermal state: crustal models (S1-S5)

The results of the thermal modelling (Fig. 4) are initially discussed, considering different heat flux variations at the crust/mantle interface (20, 40, and 60 mW/m^2), while keeping depth and thermal setting constant (S3 mean thermal conductivity values) (Figs. 5, 6, and 7). As depicted in Figs. 5, 6 and 7, at constant depths (1000, 2000 and 3000 m b.g.l., respectively), an increase in the thermal flux constrained at the crust/mantle interface results in higher expected temperatures. The primary thermal anomalies are recognized in the proximity of the eastern sector, while the lowest temperatures are observed along the Tyrrhenian side, up to the first 2000 metres of depth, and in the northern area from 3000 metres onwards. This feature is interpreted as resulting from the Moho morphology (Fig. 3e) (used as the lower boundary condition) and the superimposed thermal blanketing effects of the thick Paleogene-Quaternary deposits (Fig. 3b). The positive thermal anomaly is located beneath the sedimentary basins along the Ionian coast, whereas colder conditions are modelled in the Pollino carbonate massif area across the northern domains. It is noted that these effects are no longer visible at depths deeper than 10 km. At such depth levels, variations in the thermal field are smoother, primarily reflecting the topology of this boundary (Fig. 3d). The different hypothesized thermal settings (reported in *session 4b*) at constant depths (2000 m b.g.l.) and heat flux (20 mW/m^2) show a consistent steady thermal trend, consistent with the previously observed thermal anomalies. Maximum values are found for minimum thermal values and vice versa. Settings **4** and **5**, which assign different thermal weights to the carbonate and crystalline units, do not produce significant variations, except for the uniformity of

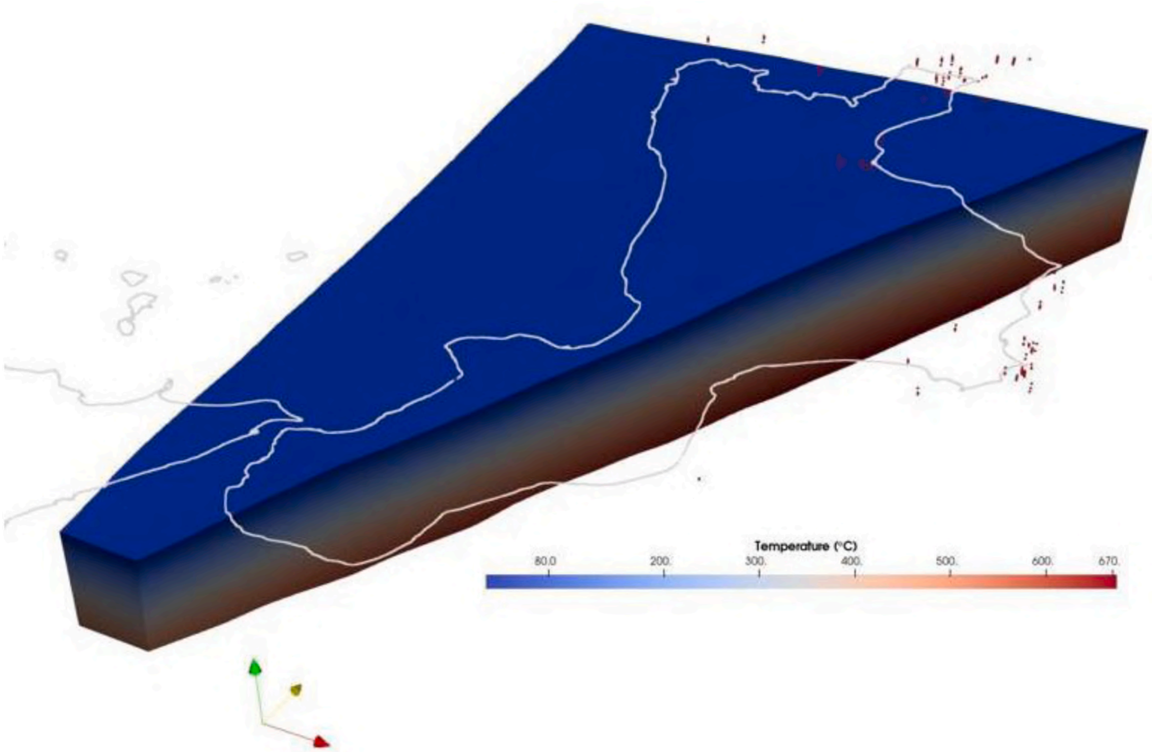

Fig. 4. 3D Temperature section of the modelled area for setting 5, assuming a heat flux of 40 mW/m^2 at the crust-mantle boundary.

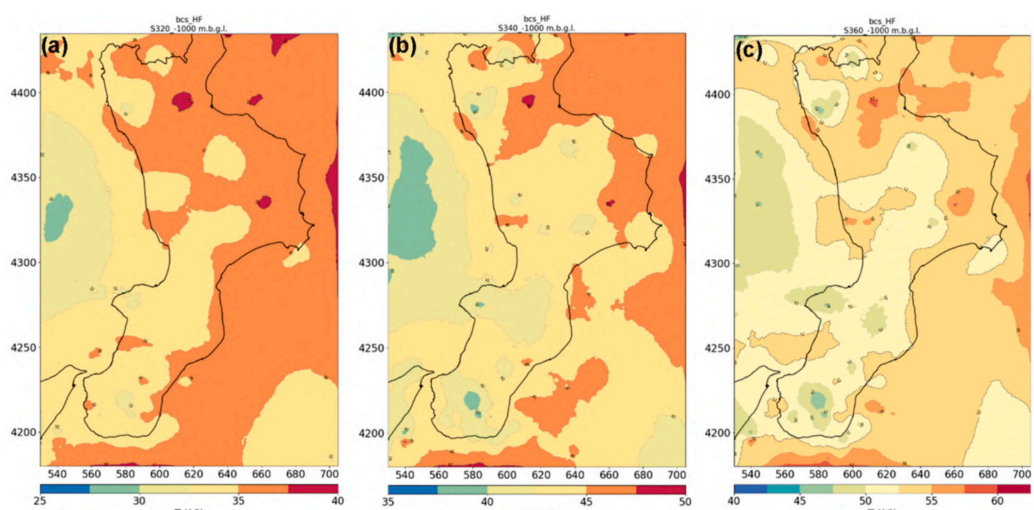

Fig. 5. Temperature maps at 1 km depth below ground level (b.g.l.) for setting 3 (mean thermal conductivity values) assuming different heat flux values at (a) 20 mW/m^2, (b) 40 mW/m^2 and (c) 60 mW/m^2 at the crust-mantle boundary (Moho). Coordinates are in EPSG:32633 – WGS84/UTM zone 33N.

thermal anomalies along the central sector of the CPO. The heat distribution in the shallow crust is primarily controlled by the properties of the low-conductivity sedimentary rocks at the top of the stratigraphic succession. This blanketing effect is especially relevant beneath areas covered by the thick succession of the Paleogene-Quaternary deposits of the orogenic units (e.g. Ionian Basins), located above a thickened highly radiogenic crust. There, the temperature gradient is higher than in the other domains of the region. On the other hand, high altitude domains (i.e., the Sila, Aspromonte and Pollino Massifs) hold a more conductive basement that facilitates efficient heat transfer, finally resulting in lower shallow temperatures.

5.2. Calibration against shallow temperature measurements (1–4 km below ground level)

All different models provide a coherent depiction of the crustal thermal configuration in terms of its regional trends. However, variations in thermal rock properties result in local differences in the obtained temperature magnitudes at shallow, sedimentary depths. The regional scale of the model limits the resolution of details regarding local lithostratigraphic variations mapped in the Calabrian sedimentary sequences. While these local structural features do not significantly affect the first-order regional thermal configuration, they are likely to exert control on a more local scale, such as the scale of direct temperature

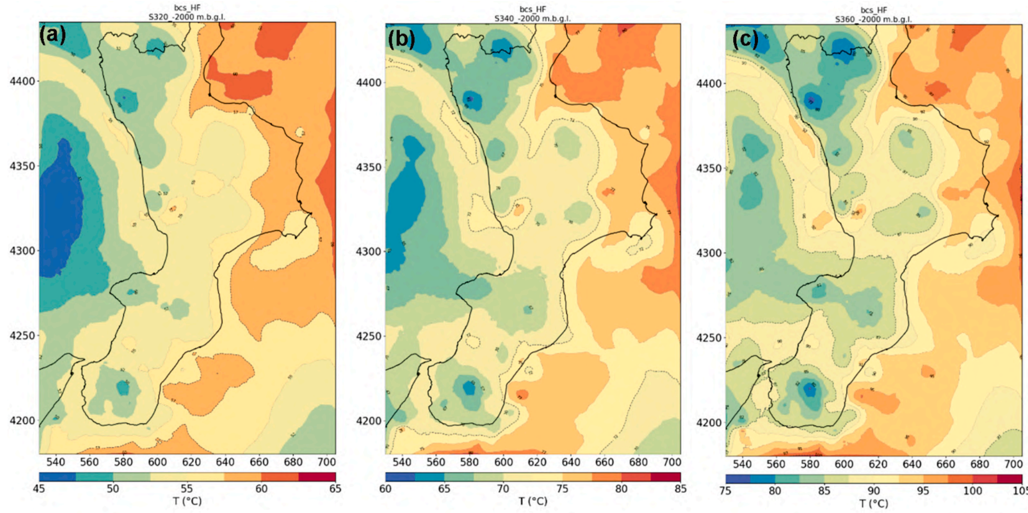

Fig. 6. Temperature maps at 2 km depth below ground level (b.g.l.) for setting 3 (mean thermal conductivity values), assuming different heat flux values at (a) 20 mW/m^2, (b) 40 mW/m^2 and (c) 60 mW/m^2 at the crust-mantle boundary (Moho). Coordinates are in EPSG:32633 – WGS84/UTM zone 33N.

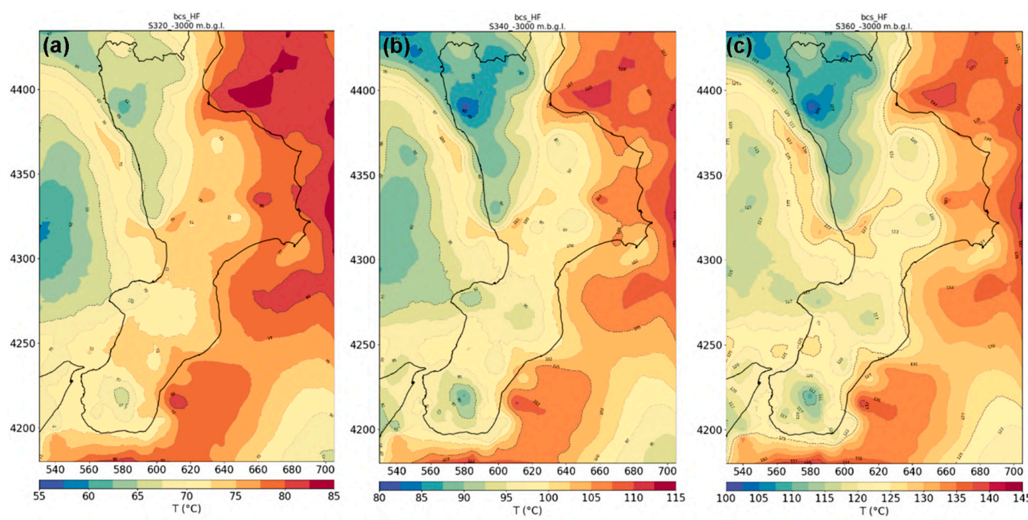

Fig. 7. Temperature maps at 3 km depth below ground level (b.g.l.) for setting 3 (mean thermal conductivity values), assuming different heat flux values at (a) 20 mW/m^2, (b) 40 mW/m^2 and (c) 60 mW/m^2 at the crust-mantle boundary (Moho). Coordinates are in EPSG:32633 – WGS84/UTM zone 33N.

measurements. Model calibration is performed by comparing the extrapolated data from each model against a dataset of measured temperatures available from the Italian National Geothermal Database (Cataldi et al., 1995; Trumpy and Manzella, 2017). The public dataset for Calabria (and partially for Basilicata) comprises 254 temperature data points from 45 wells drilled from the surface down to 4 km b.g.l. [Measurements and bottom hole temperature were corrected using the Squarci-Taffi empirical method (Della Vedova et al., 2001), where temperatures are extrapolated with a homogeneous gradient] (Fig. 1). This data-oriented calibration introduces an epistemic bias due to an uneven distribution of available measurements and a lack of resolution of local stratigraphy. The goal is to identify the set of properties within the structural resolution of the input geological model that provides the best fit to the available measurements, and to derive implications for the shallow geothermal potential of the study area. To examine the local thermal configuration, theoretical temperatures (calculated at different depths with different thermal fluxes and settings) were compared with temperatures measured in the well using binary graphs. Additionally, the Root Mean Square Error (in°C) has been computed for each model as a function of depth to assess the suitability of the results (Figs. 8, 9, and 10). The temperature derived from the Crustal Model with a heat flux of 60 mW/m^2 showed the lowest correlations with the measured temperatures, with a general overestimation (up to 100°C) of expected temperatures. On the other hand, the models based on heat fluxes of 40 mW/m^2 (for S3 "mean values") and 20 mW/m^2 (for all applied settings) showed a perfect correlation, with errors often below 10°C. A common feature across all sub-settings reported in Fig. 8 (heat flux of 20 mW/m^2) is that the modelled temperature area slightly underestimates the measurements, with a maximum error of about 35°C at depths up to 4 km. The underestimation trend in the observations could be related to the chosen boundary condition, which assumes a constant heat flux at the base of the model. The imposed 20 mW/m^2 value has been treated as an average across the entire lower boundary of the model, likely providing a conservative estimate of the actual crustal heat flow beneath specific domains. In these contexts, higher crustal heat flow would be expected, leading to higher temperatures that better agree with the measurements. Overall, the models based on 20 mW/m^2 (Fig. 8) show the best correlations, suggesting an average flux that does not deviate considerably from the assumed values. An additional step that would enable detailed assessment of any thermal anomalies involves studying

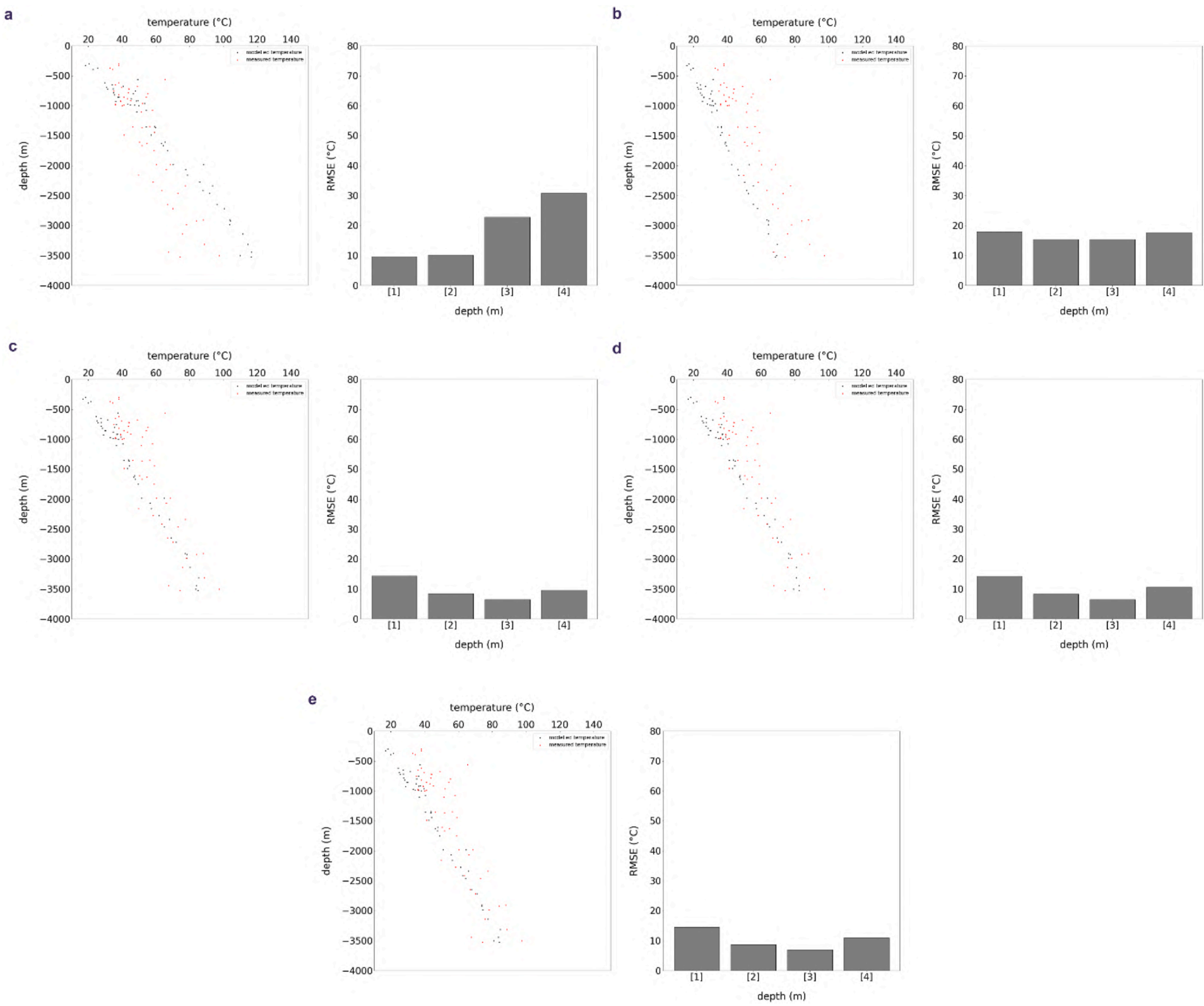

Fig. 8. Temperatures modelled (black points) vs. measured (red points) for Crust/Moho thermal flow rates of 20 mW/m^2. (a) setting 1 (min thermal conductivity values); (b) setting 2 (max thermal conductivity values); (c) setting 3 (mean thermal conductivity values); (d) setting 4 (mean thermal conductivity values and max values for the Mesozoic Units); (e) setting 5 (mean thermal conductivity values and max values for the Crystalline Units). The temperature comparisons are associated with the graph showing the Root Mean Square Error expressed in (°C) for different depth ranges expressed in meters (1 = [0 - -1000]; 2 = [-1000 - -2000]; 3 = [-2000 - -3000]; 4 = [-3000 - -4000]).

the spatial variation of thermal fluxes at the Moho/crust interface. Further evidence for the proposed model is provided by the works of Apollaro et al. (2020) and Vespasiano et al. (2023), and references therein, which use powerful geothermometric functions and geothermometric modelling approaches applied to Calabrian geothermal fluids to determine the relative temperatures of the main regional geothermal systems. For depths between 1.5 and 2.5 km b.g.l., the authors proposed reservoir temperatures between 50 and 90°C, which are comparable to those predicted by the theoretical model.

5.3. Geodynamic considerations

The Calabria region occupies a key position within the central Mediterranean geodynamic framework, representing a segment of the Alpine-Apennine-Maghrebian orogenic system characterized by complex lithospheric interactions. The arcuate structure of the Calabria-Peloritani Orogen (CPO), shaped by Cenozoic convergence and retreating subduction, results in a lithospheric architecture marked by alternating crustal domains, inherited tectono-metamorphic units, and a variable Moho depth. These geodynamic features exert a first-order control on the regional thermal regime. The 3D thermal modelling performed in this study captures the influence of major geodynamic features such as the flexural geometry of the subducting slab and the crustal thinning beneath the Ionian and Tyrrhenian domains. The model results highlight lateral temperature variations driven by both lithological heterogeneity and the morphology of the Moho, with elevated temperatures localized beneath sediment-filled extensional basins along the Ionian margin. This pattern reflects the combined effect of sedimentary blanketing, reduced thermal conductivity in the upper crust, and increased mantle-derived heat flow due to lithospheric thinning. Furthermore, the tectonic segmentation between the northern carbonate-dominated and southern crystalline domains, delineated by crustal-scale structures such as the Catanzaro and Palmi Lines, is mirrored in the modelled thermal field. These inherited tectonic discontinuities likely act not only as structural boundaries but also as potential zones of enhanced permeability and fluid flow, which may locally modify the heat transport regime through advective processes. In this context, there is evidence of prevalent thermalism such as the Caronte system in the northern portions of the Catanzaro Strait, the Crotonese system (eastern sector of northern Calabria), the Cerchiara system (northern Calabria in proximity of the Pollino tectonic system), the Guardia Piemontese thermal system (Coastal Chain), Galatro and

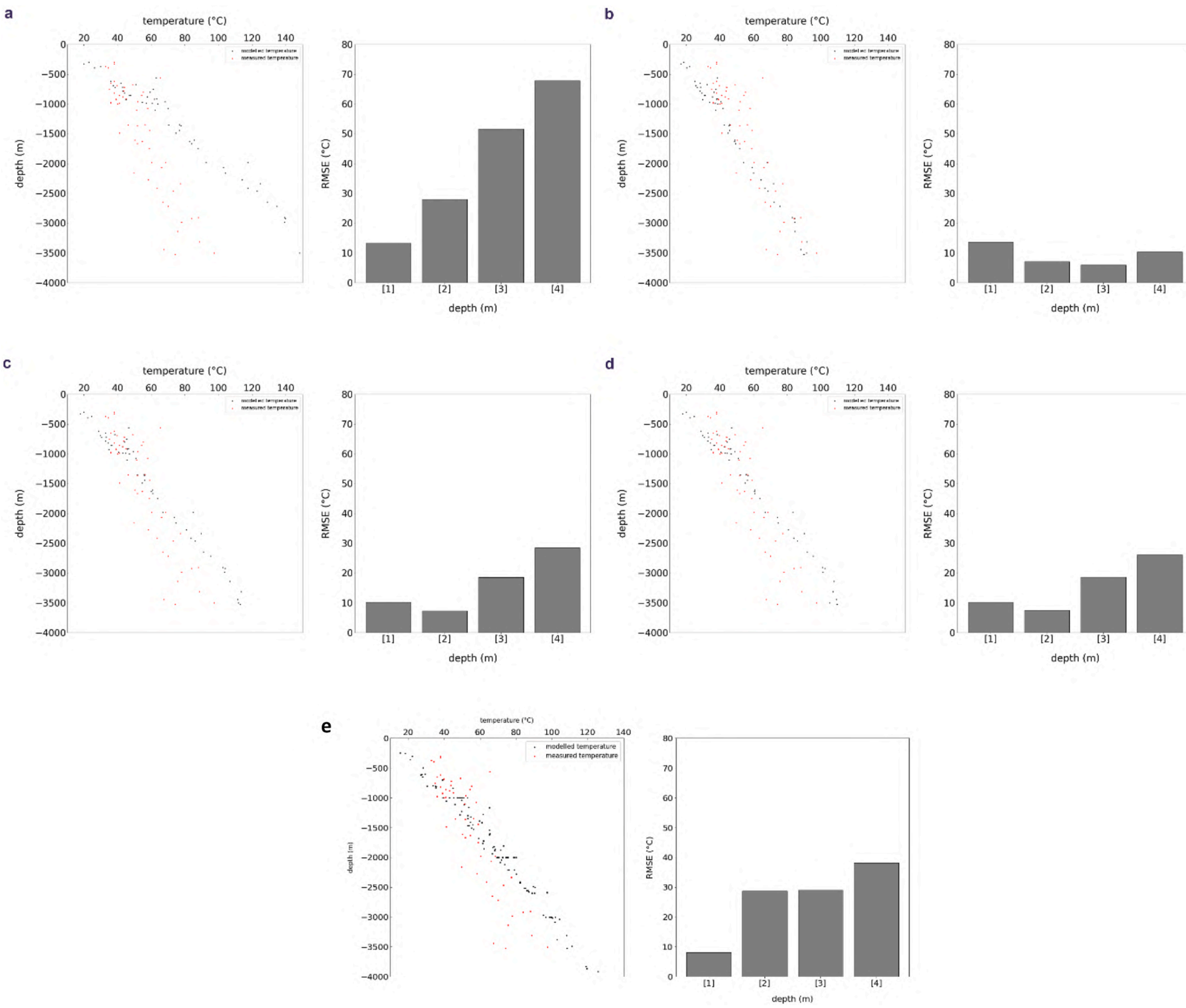

Fig. 9. Temperatures modelled (black points) vs. measured (red points) for Crust/Moho thermal flow rates of 40 mW/m^2. (a) setting 1 (min thermal conductivity values); (b) setting 2 (max thermal conductivity values); (c) setting 3 (mean thermal conductivity values); (d) setting 4 (mean thermal conductivity values and max values for the Mesozoic Units); (e) setting 5 (mean thermal conductivity values and max values for the Crystalline Units). The temperature comparisons are associated with the graph showing the Root Mean Square Error expressed in (°C) for different depth ranges expressed in meters (1 = [0 - -1000]; 2 = [-1000 - -2000]; 3 = [-2000 - -3000]; 4 = [-3000 - -4000]).

Antonimina systems (western and eastern sectors, respectively of the Serre massif in proximity of the Palmi and Nicotera tectonic systems). For these systems, Apollaro et al., 2020 and Vespasiano et al., 2023 provided reservoir depth and temperature respectively of 1.5 km and 55 ± 6°C for the Caronte system, 1.8 km and 65°C for the Crotonese system, 1 km and 38°C for the Cerchiara system, 1.4 km and 60°C for the Guardia Piemontese and 2 km and 69 ± 15°C for the Galatro systems. These temperature values are strongly consistent with the temperature values derived from the theoretical model.

It should be emphasized that the proposed model has some limitations, mainly related to the distribution of the available geological and geophysical data. Specifically, while the eastern sector shows a good areal distribution of deep wells used to validate the thermal model (e.g., VIDEPI and CROP projects (Scrocca, 2003) as reported in Fig. 1), the Tyrrhenian sector is characterized by an extremely poor distribution of deep boreholes and seismic profiles. The scarcity of data, especially in offshore areas, weakly constrains the model results. Moreover, in the Tyrrhenian sector, we did not consider the magmatic bodies associated with the Aeolian arc and the localized thermal anomalies in the distal areas of Capo Vaticano (De Ritis et al., 2010). These limitations make the model for the onshore (continental) portions more tightly constrained than for the deep Tyrrhenian portions.

Furthermore, while the current steady-state conductive model provides a robust framework for assessing regional-scale geothermal gradients, future work should explore transient and coupled thermal-hydraulic simulations to account for the temporal evolution of heat flow and the role of deep fluid circulation. Such approaches will be critical for fully resolving the thermal signatures of geodynamically active domains and for improving geothermal resource assessments in structurally complex regions.

6. Conclusions

The methods presented in this research aim to precisely characterize the thermal configuration of the Calabrian subsurface, thereby establishing a foundation for the potential exploitation of geothermal energy in the region. Our multidisciplinary approach to the geothermal characterization involved a two-stage process: a 3D geological reconstruction followed by thermal numerical simulations. By applying multiple boundary conditions and accounting for heat input from below, we successfully obtained the steady-state thermal field.

Our numerical simulations, conducted under varying thermal boundary conditions, provide a robust and detailed depiction of the regional thermal structure. The results show that temperature anomalies

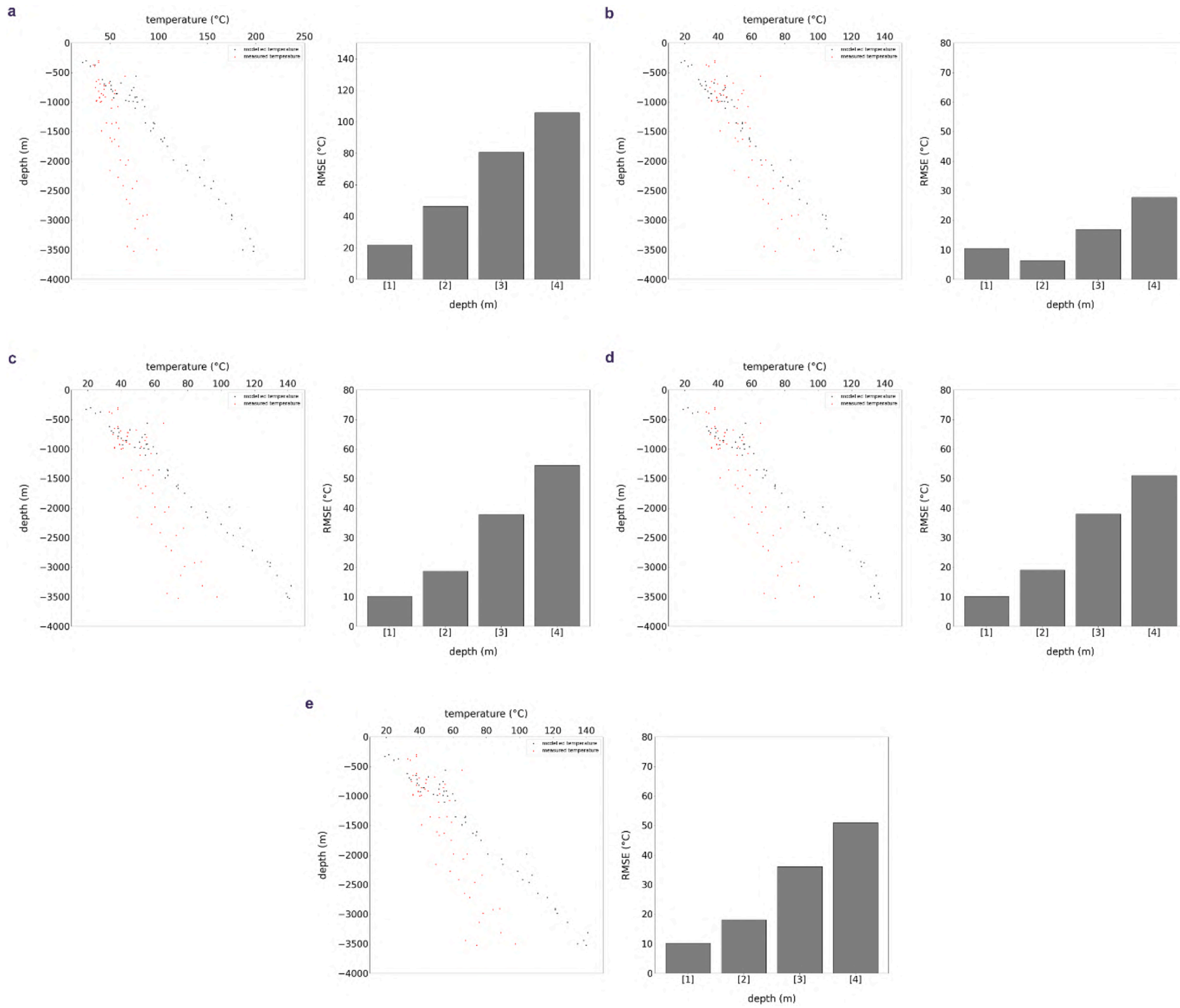

Fig. 10. Temperatures modelled (black points) vs. measured (red points) for Crust/Moho thermal flow rates of 60 mW/m^2. (a) setting 1 (min thermal conductivity values); (b) setting 2 (max thermal conductivity values); (c) setting 3 (mean thermal conductivity values); (d) setting 4 (mean thermal conductivity values and max values for the Mesozoic Units); (e) setting 5 (mean thermal conductivity values and max values for the Crystalline Units). The temperature comparisons are associated with the graph showing the Root Mean Square Error expressed in (°C) for different depth ranges expressed in meters (1 = [0 - -1000]; 2 = [-1000 - -2000]; 3 = [-2000 - -3000]; 4 = [-3000 - -4000]).

are strongly influenced by sedimentary blanketing, crustal architecture, and variations in Moho depth. Model calibration, performed with 254 well-temperature data points, demonstrates good agreement under average-to-conservative basal heat flux conditions. However, discrepancies in shallow temperatures highlight the need to incorporate advective processes into future simulations.

The findings identify widespread zones favourable for low-to-medium enthalpy geothermal energy at depths of 1-3 km, particularly within the sedimentary basins along the Ionian margin. While this approach does not resolve deep high-enthalpy targets, it establishes a valuable baseline for future investigations using transient and coupled thermal-hydraulic models. While research into Calabria's geothermal potential consistently identifies carbonate units as the principal reservoir, our model suggests that other formations within both the sedimentary cover and the crystalline basement may also constitute significant geothermal systems that warrant further detailed investigation.

A notable observation is that the thermal conductivity values assigned to the primary sedimentary rocks consistently overestimate shallow temperature measurements, regardless of the applied lower boundary condition. This discrepancy points to the presence of additional, unmodeled processes - such as coupled heat and fluid transport - underscoring the need for further research. Significantly, the entire region exhibits temperature conditions at shallow depths (1000–2000 meters) that are suitable for low-enthalpy geothermal energy exploitation or direct heat utilization, such as with geothermal heat pumps. Conversely, thermal conditions at depths exceeding 10 km appear to be predominantly controlled by mantle heat flow and radiogenic heat production within the crystalline basement rocks.

The advances presented here have the potential to significantly improve the spatial resolution and accuracy of regional geothermal data, which are currently limited. These findings are particularly relevant in the context of the current social and political situation and the evolving energy market dynamics, offering a pathway to accelerate the transition toward more sustainable exploitation of subsurface heat as a renewable energy resource. The next step will be to select high-interest pilot areas and develop site-specific models that account for both the role of fluids and the influence of tectonic structures on overall heat transport.

CRediT authorship contribution statement

G. Vespasiano: Writing – review & editing, Writing – original draft, Visualization, Validation, Software, Resources, Methodology, Investigation, Formal analysis, Data curation, Conceptualization. **G. Floridia:** Writing – review & editing, Writing – original draft, Visualization, Validation, Software, Methodology, Investigation, Formal analysis, Data curation, Conceptualization. **M. Giuffrida:** Writing – review & editing, Methodology, Investigation, Data curation. **M. Viccaro:** Writing – review & editing, Supervision, Data curation, Conceptualization, Validation, Writing – original draft. **A. Bloise:** Writing – review & editing, Validation, Supervision, Data curation, Writing – original draft. **R. De Rosa:** Writing – review & editing, Validation, Supervision, Project administration, Funding acquisition, Conceptualization, Data curation, Writing – original draft. **M. Cacace:** Writing – review & editing, Software, Methodology, Investigation, Data curation, Formal analysis, Writing – original draft. **I. Fuoco:** Writing – review & editing, Methodology, Formal analysis, Data curation, Software, Writing – original draft. **M.F. La Russa:** Writing – review & editing, Validation, Supervision, Data curation, Writing – original draft. **F. Muto:** Writing – review & editing, Validation, Supervision, Investigation. **R. Dominici:** Writing – review & editing, Validation, Supervision, Investigation. **L. Russo:** Writing – review & editing, Visualization, Methodology, Data curation, Formal analysis, Software. **M. Cipriani:** Writing – review & editing, Software, Methodology, Data curation, Formal analysis, Writing – original draft. **A. Guido:** Writing – review & editing, Validation, Supervision, Data curation, Writing – original draft. **G. Maruca:** Writing – review & editing, Software, Methodology, Data curation, Formal analysis, Writing – original draft. **C. Apollaro:** Writing – review & editing, Writing – original draft, Validation, Supervision, Resources, Project administration, Funding acquisition, Formal analysis, Data curation, Conceptualization, Investigation, Methodology, Software.

Declaration of competing interest

The authors declare that they have no known competing financial interests or personal relationships that could have appeared to influence the work reported in this paper.

Acknowledgments

This work was funded by the Next Generation EU - Italian NRRP, Mission 4, Component 2, Investment 1.5, call for the creation and strengthening of ‘Innovation Ecosystems’, building ‘Territorial R&D Leaders’ (Directorial Decree n. 2021/3277) - project Tech4You - Technologies for climate change adaptation and quality of life improvement, n. ECS0000009. This work reflects only the authors’ views and opinions; neither the Ministry for University and Research nor the European Commission can be considered responsible for them.

Supplementary materials

Supplementary material associated with this article can be found, in the online version, at doi:10.1016/j.geothermics.2026.103604.

Data availability

Data will be made available on request.

References

Abate, S., Angelino, A., Balasco, M., Botteghi, S., Bruno, P., Caielli, G., Caputi, A., Cardellicchio, N., Catalano, R., Contino, A., 2014. VIGOR: Sviluppo geotermico nella regione Sicilia – Studi di fattibilità a Mazara del Vallo e Termini Imerese. Valutazione geotermica con geofisica elitrasportata. https://doi.org/10.13140/RG.2.1.4496.7449.

Akimbekova, A., Carboni, F., Mancinelli, P., Barreca, G., Scarfì, L., Pauselli, C., Monaco, C., Barchi, M.R., 2023. Gravity modelling of the Tyrrhenian-Calabrian-Ionian subduction system. Front. Earth Sci. 11, 1259831.

Alçiçek, H., Bülbül, A., Yavuzer, İ., Alçiçek, M.C., 2019. Origin and evolution of the thermal waters from the Pamukkale Geothermal Field (Denizli Basin, SW Anatolia, Turkey): Insights from hydrogeochemistry and geothermometry. J. Volcanol. Geotherm. Res. 372, 48–70.

Amodio Morelli, L., Bonardi, G., Colonna, V., Dietrich, D., Giunta, G., Ippolito, F., Liguori, V., Lorenzoni, S., Paglionico, A., Perrone, V., Piccarreta, G., Russo, M., Scandone, P., Zanettin-Lorenzoni, E., Zuppetta, A., 1976. L’arco calabro-peloritano nell’orogene appenninico-maghrebide, 17. Memorie della Società Geologica Italiana, pp. 1–60.

Apollaro, C., Tripodi, V., Vespasiano, G., De Rosa, R., Dotsika, E., Fuoco, I., Critelli, S., Muto, F., 2019. Chemical, isotopic and geotectonic relations of the warm and cold waters of the Galatro and Antonimina thermal areas, southern Calabria, Italy. Mar. Pet. Geol. 109, 469–483. https://doi.org/10.1016/j.marpetgeo.2019.06.020.

Apollaro, C., Caracausi, A., Paternoster, M., Randazzo, P., Aiuppa, A., De Rosa, R., Fuoco, I., Mongelli, G., Muto, F., Vannia, E., Vespasiano, G., 2020. Fluid geochemistry in a low-enthalpy geothermal field along a sector of southern Apennines chain (Italy). J. Geochem. Explor. https://doi.org/10.1016/j.gexplo.2020.106618.

Apollaro, C., Dotsika, E., Marini, L., Barca, D., Bloise, A., De Rosa, R., Doveri, M., Lelli, M., Muto, F., 2012. Chemical and isotopic characterization of the thermomineral water of Terme Sibarite springs (Northern Calabria, Italy). Geochem. J. 46, 117–129.

Apollaro, C., Vespasiano, G., Fuoco, I., Taussi, M., De Rosa, R., La Russa, M.F., Guido, A., Di Curcio, D., Renzulli, A., Russo, L., Ciniglia, F., D’Amico, F., Cipriani, M., Maruca, G., Virgili, G., Bloise, A., 2025. Impact and evaluation of potential implications of coastal plains on soil greenhouse gas emissions: insights from the Sibari Coastal Plain (Calabria, Southern Italy). Sci. Total Environ. 964, 178611.

Apollaro, C., Vespasiano, G., Fuoco, I., Taussi, M., De Rosa, R., La Russa, M.F., Bloise, A., 2025. Impact and evaluation of potential implications of coastal plains on soil greenhouse gas emissions: insights from the Sibari Coastal Plain (Calabria, Southern Italy). Sci. Total Environ. 964, 178611.

Apollaro, C., Vespasiano, G., Muto, F., De Rosa, R., Barca, D., Marini, L., 2016. Use of mean residence time of water, flowrate, and equilibrium temperature indicated by water geothermometers to rank geothermal resources. Application to the thermal water circuits of Northern Calabria. J. Volcanol. Geotherm. Res. 328, 147–158.

Atzori, P., Cirrincione, R., Del Moro, A., Mazzoleni, P., 2000. Petrogenesis of late Hercynian calc-alkaline dykes of mid-eastern Sardinia: petrographical and geochemical data constraining hybridization process. Eur. J. Mineral. 12 (6), 1261–1282.

Barberi, G., Cosentino, M.T., Gervasi, A., Guerra, I., Neri, G., Orecchio, B., 2004. Crustal seismic tomography in the Calabrian Arc region, south Italy. Phys. Earth Planet. Inter. 147 (4), 297–314.

Basilici, M., Mazzoli, S., Megna, A., Santini, S., Tavani, S., 2019. Geothermal Model of the Shallow Crustal Structure across the "Mountain Front Fault" in Western Lurestan, Zagros Thrust Belt Iran. Geosciences 9, 301. https://doi.org/10.3390/geosciences9070301.

Basilici, M., Mazzoli, S., Megna, A., Santini, S., Tavani, S., 2020. 3-D Geothermal Model of the Lurestan Sector of the Zagros Thrust Belt, Iran. Energies 13, 2140. https://doi.org/10.3390/en13092140.

Bencini, A., Ciracò, G., 1982. Caratteristiche geochimiche di alcune acque termali della provincia di Catanzaro. Rend. SIMP 38, 1189–1195.

Birgel, D., Guido, A., Liu, X., Hinrichs, K., Gier, S., Peckmann, J., 2014. Hypersaline conditions during deposition of the Calcare di Base revealed from archaeal di- and tetraether inventories. Org. Geochem. 77, 11–21.

Bonardi, G., Compagnoni, R., Messina, A., Perrone, V., 1984a. Riequilibrazioni metamorfiche di probabile eta alpina nell’Unita dell’Aspromonte– Arco Calabro Peloritano. Rend. Soc. Ital. Mineral. Petrol. 39, 613–628.

Bonardi, G., Compagnoni, R., Messina, A., Perrone, V., Russo, S., De Francesco, A.M., Del Moro, A., Platt, J., 1992. Sovrimpronta metamorfica alpina nell’Unità dell’aspromonte (settore meridionale dell’Arco Calabro-Peloritano), 111. Bollettino della Società Geologia Italiana, pp. 81–108.

Bonardi, G., Giunta, G., Perrone, V., Russo, M., Zuppetta, A., Ciampo, G., 1980. Osservazioni Sull’evoluzione Dell’arco Calabro-Peloritano Nel Miocene Inferiore: La Formazione Di Stilo-Capo D’orlando, 99. Bollettino della Società Geologica Italiana, pp. 365–393.

Bonardi, G., Messina, A., Perrone, V., Russo, S., Zuppetta, A., 1984b. L’unita di Stilo nel settore meridionale dell’Arco Calabro-Peloritano, 103. Bollettino della Società Geologica Italiana, pp. 279–309.

Brandt, S., Schenk, V., 2020. Metamorphic Response to Alpine Thrusting of a Crustal-scale Basement Nappe in Southern Calabria (Italy). In J. Petrol. 61 (11-12). https://doi.org/10.1093/petrology/egaa063. Article egaa063.

Brunetti, M., Maugeri, M., Nanni, T., Simolo, C., Spinoni, J., 2014. High-resolution temperature climatology for Italy: Interpolation method intercomparison. Int. J. Climatol. 34 (4), 1278–1296. https://doi.org/10.1002/joc.3764. Number.

Cacace, M., Jacquey, A.B., 2017. Flexible parallel implicit modelling of coupled thermal–hydraulic–mechanical processes in fractured rocks. Solid Earth 8, 921–941. https://doi.org/10.5194/se-8-921-2017.

Calcara, M., Quattrocchi, F., 1993. Sulla Scelta di Siti Idonei al Monitoraggio Geochimico ai Fini Della Sorveglianza Sisimica Della Calabria Settentrionale: Valle Crati⁄Piana di Sibari. Atti Convegno Naz. GNGTS.

Calò, M., Dorbath, C., Luzio, D., Rotolo, S.G., D'anna, G., 2012. Seismic velocity structures of southern Italy from tomographic imaging of the Ionian slab and petrological inferences. Geophys. J. Int. 191 (2), 751–764.

Caracausi, A., Ditta, M., Italiano, F., Longo, M., Nuccio, P.M., Paonita, A., Rizzo, A., 2005. Changes in fluid geochemistry and physico-chemical conditions of geothermal systems caused by magmatic input: The recent abrupt outgassing off the island of Panarea (Aeolian Islands, Italy). Geochim. Cosmochim. Acta 69 (12), 3045–3059.

Carminati, E., Lustrino, M., Cuffaro, M., Doglioni, C., 2010. Tectonics, magmatism and geodynamics of Italy: What we know and what we imagine. Journal of the Virtual Explorer, Electronic Edition. In: Beltrando, M., Peccerillo, A., Mattei, M., Conticelli, S., Doglioni, C. (Eds.), The Geology of Italy: tectonics and life along plate margins, pp. 36–39.

Cassano, E., Fichera, R., Arisi Rota, F., 1986. Rilievo aeromagnetico d'Italia. Alcuni risultati interpretativi. Atti del 5, 939–958.

Cataldi, R., Mongelli, F., Squarci, P., Taffi, L., Zito, G., Calore, C., 1995. Geothermal ranking of Italian territory. Geothermics 24 (1), 115–129.

Cavazza, W., Ingersoll, R.V., 2005. Detrital modes of the ionian forearc basin fill (oligocenequaternary) reflect the tectonic evolution of the calabria-peloritani terrane (southern Italy). J. Sediment. Res. 75 (2), 268–279.

Cello, G., Invernizzi, C., Mazzoli, S., 1996. Structural signature of tectonic processes in the Calabrian Arc, southern Italy: Evidence from the oceanic-derived Diamante-Terranova Unit. Tectonics 15 (1), 187–200.

Cello, G., Tortorici, L., Turco, E., Guerra, I., 1981. Profili profondi in Calabria settentrionale. Boll. Soc. Geol. Ital. 100 (4), 423–431.

Cifelli, F., Mattei, M., Della Seta, M., 2008. Calabrian Arc oroclinal bending: the role of subduction. Tectonics 27 (5) art. no. TC5001.

Cipriani, M., Costanzo, A., Feely, M., Guido, A., D'Antonio, M., Vespasiano, G., Donato, S., Cianflone, G., Maruca, G., Apollaro, C., Alessandro, F., Perri, F., Dominici, R., 2026. The Messinian halite facies: insights into halite crystallisation and depositional environments using geochemical, petrographic and fluid inclusion studies. Geosci. Front. https://doi.org/10.1016/j.gsf.2025.102207.

Cipriani, M., Donato, S., Alessandro, F., Campilongo, G., Cianflone, G., Costanzo, A., Guido, A., Lanzafame, G., Magarò, P., Maletta, C., Maruca, G., Dominici, R., 2024. Can crystal imperfections alter the petrophysical properties of halite minerals? Mar. Pet. Geol. 168 (1), 107013. https://doi.org/10.1016/j.marpetgeo.2024.107013.

Cirrincione, R., 1996. Geochronologic and petrologic features of porphyrite rocks in the Tortonian conglomerate of north-eastern Sicily: hypothesis on their provenance. Period. Mineral. 65 (1-2), 21–33.

Cirrincione, R., Pezzino, A., 1991. Caratteri strutturali dell'evento alpino nella serie mesozoica di Ali e nella Unita metamorfica di Mandanici (Peloritani orientali), 47. Memorie della Società Geologica Italiana, pp. 263–272.

Cirrincione, R., Fazio, E., Fiannacca, P., Ortolano, G., Pezzino, A., Punturo, R., 2008. Petrological and microstructural constraints for orogenetic exhumation modelling of HP rocks: The example of southern Calabria Peloritani Orogen (Western Mediterranean). In: GeoMod 2008, Third International Geomodelling Conference, Firenze, 22-24 September 2008. Bollettino di Geofisica Teorica e Applicata, 49, pp. 141–146.

Cirrincione, R., Fazio, E., Ortolano, G., Pezzino, A., Punturo, R., 2012. Fault-related rocks: Deciphering the structural-metamorphic evolution of an accretionary wedge in a collisional belt. NE Sicily, Int. Geol. Rev. 54, 940–956.

Cirrincione, R., Fazio, E., Fiannacca, P., Ortolano, G., Pezzino, A., Punturo, R., 2015. The Calabria-Peloritani Orogen, a composite terrane in Central Mediterranean; its overall architecture and geodynamic significance for a pre-Alpine scenario around the Tethyan basin. Period. Mineral. 84 (3B), 701–749.

Clauser, C., Huenges, E., 1995. Thermal conductivity of rocks and minerals. Rock Phys. Ph. Relat.: Handb. Phys. Constants 3, 105–126.

Cristofolini, R., Ghisetti, F., Scarpa, R., Vezzani, L., 1985. Character of the stress field in the Calabrian arc and southern Apennines (Italy) as deduced by geological, seismological and volcanological information. Tectonophysics 117 (1-2), 39–58.

De Ritis, R., Dominici, R., Ventura, G., Nicolosi, I., Chiappini, M., Speranza, F., De Rosa, R., Donato, P., Sonnino, M., 2010. A buried volcano in the Calabrian Arc (Italy) revealed by high-resolution aeromagnetic data. J. Geophys. Res.: Solid Earth 115 (B11).

Della Vedova, B., Bellani, S., Pellis, G., Squarci, P., 2001. Deep temperatures and surface heat flow distribution. In: Vai, G.B., Martini, I.P. (Eds.), Anatomy of an orogen: the Apennines and adjacent Mediterranean basins. Kluwer, Dordrecht, pp. 65–76.

Di Sipio, E., Galgaro, A., Destro, E., Giaretta, A., Chiesa, S., Team, V., 2013. Thermal conductivity of rocks and regional mapping. In: Proceedings of European Geothermal Conference 2013.

Di Sipio, E., Galgaro, A., Destro, E., Teza, G., Chiesa, S., Giaretta, A., Manzella, A., 2014. Subsurface thermal conductivity assessment in Calabria (southern Italy): a regional case study. Environ. Earth Sci. 72, 1383–1401.

Di Stefano, R., Ciaccio, M.G., 2014. The lithosphere and asthenosphere system in Italy as inferred from the Vp and Vs 3D velocity model and Moho map. J. Geodyn. 82, 16–25.

Dietrich, F., 1988. Sense of overthrusth shear in the Alpine nappes of Calabria (Southern Italy). J. Struct. Geol. 10, 373–381.

Dominici, R., Costanzo, A., Guido, A., Maruca, G:, Perri, F., Molinaro, D., Cipriani, M., 2025. Short-Term Climate Oscillations During the Messinian Salinity Crisis: New Insights from Gypsum Lithofacies of the Crati Basin (Lattarico, Calabria, Southern Italy). Minerals 15, 542. https://doi.org/10.3390/min15050542.

Duchi, V., Bencini, A., Cortese, G., Minissale, A., 1991. Caratteristiche geochimiche dei fluidi della Calabria centro settentrionale e loro potenzialità geotermiche. Boll. Soc. Geol. It. 110, 273–280.

Fazio, E., Cirrincione, R., Pezzino, A., 2008. Estimating P-T conditions of Alpine-type metamorphism using multistage garnet in the tectonic windows of the Cardeto area (southern Aspromonte Massif, Calabria). Mineral Petrol. 93, 111–142.

Fichtner, A., van Herwaarden, D.P., Afanasiev, M., Simutė, S., Krischer, L., Çubuk-Sabuncu, Y., Taymaz, T., Colli, L., Saygin, E., Villaseñor, A., Trampert, J., Cupillard, P., Bunge, H., Igel, H., 2018. The collaborative seismic earth model: generation 1. Geophys. Res. Lett. 45 (9), 4007–4016.

Floridia, G., Cacace, M., Scheck-Wenderoth, M., Bott, J., Viccaro, M., 2022. 3D thermal model of Sicily (Southern Italy) and perspectives for new exploration campaigns for geothermal resources. Glob. Planet. Change 218, 103976.

Galgaro, A., Di Sipio, E., Destro, E., Chiesa, S., Uricchio, V.F., Bruno, D., Masciale, R., Lopez, N., Iaquinta, P., Teza, G., Iovine, G., Montanari, Manzella, D.A., Soleri, S., Greco, R., Di Bella, G., Monteleone, S., Sabatino, M., Iorio, M., Petruccione, E., Giaretta, A., Tranchida, G., Trumpy, E., Gola, G., D'Arpa, S., 2012. Methodological approach for evaluating the geo-exchange potential: VIGOR Project. Acque Sotter.-Ital. J. Groundw. 1 (3).

Gardner, G.H.F., Gardner, L.W., Gregory, A.R., 1974. Formation velocity and density; the diagnostic basics for stratigraphic traps. Geophysics 39 (6), 770–780. https://doi.org/10.1190/1.1440465.

GEOTHOPICA database. 2026, http://geothopica.igg.cnr.it/.

Giuffrida, M., Floridia, G., Cacace, M., Viccaro, M., 2025. Thermal model of the Pantelleria Island (Sicily Channel, Southern Italy): new insights for promoting the sustainable exploitation of geothermal resources on the island. Geotherm. Energy 13 (1), 14.

Gola, G., Manzella, A., Trumpy, E., Montanari, D., van Wees, J.D., 2013. Deep-seated geothermal resource assessment of the VIGOR project regions. Italy Eur. Geotherm. Congr. 3–7.

Grad, M., Tiira, T., Working Group, E.S.C., 2009. The Moho depth map of the European Plate. Geophys. J. Int. 176 (1), 279–292.

Graessner, T., Schenk, V., 1999. Low-pressure metamorphism of Palaeozoic pelites in the Aspromonte, southern Calabria: constraints for the thermal evolution in the Calabrian crustal crosssection during the Variscan orogeny. J. Metamorph. Geol. 17 (2), 157–172.

Guerrera, F., Martın-Algarra, A., Perrone, V., 1993. Late Oligocene-miocene syn-late-orogenic successions in western and central mediterranean chains from the betic cordillera to the southern apennines. Terra Nova 5, 525–544.

Guido, A., Jacob, J., Gautret, P., Laggoun-Dèfarge, F., Mastandrea, A., Russo, F., 2007. Molecular fossils and other organic markers as palaeoenvironmental indicators of the Messinian Calcare di Base Formation: normal versus stressed marine deposition (Rossano Basin, northern Calabria, Italy). Palaeo3 255, 265–283.

Gurrieri, S., Hauser, S., Valenza, M., 1984. Indagine preliminare su alcune sorgenti termali della Calabria per una futura sorveglianza geochimica dell'attività sismica. Min. Petrog. Acta 28, 101–122.

Han, Suh, J., 2024. Spatial prediction of soil contaminants using a hybrid random forest–ordinary kriging model. Appl. Sci. 14 (4), 1666.

Hou, H.S., Wang, C.S., Zhang, J.D., Ma, F., Fu, W., Wang, P.J., Huang, Y-J, Zou, C., Gao, Y., Gao, Y., Zhang, L., Yang, J., Guo, R., 2018. Deep continental scientific drilling engineering project in Songliao Basin: Progress in earth science research. China Geol. 1 (2), 173–186. https://doi.org/10.1016/j.apgeochem.2019.05.011.

Iannace, A., Vitale, S., D'errico, M., Mazzoli, S., Di Staso, A., Macaione, E., Bonardi, G., 2007. The carbonate tectonic units of northern Calabria (Italy): a record of Apulian palaeomargin evolution and Miocene convergence, continental crust subduction, and exhumation of HP–LT rocks. J. Geol. Soc. 164 (6), 1165–1186.

Ietto, A., Barillaro, A.M., 1993. L'Unità di San Donato quale margine deformato cretacicopaleogenico del bacino di Lagonegro (Appennino meridionale-Arco Calabro), 111. Bollettino della Società Geologica Italiana, pp. 193–215.

Ietto, A., Ietto, F., 1998. Sviluppo e annegamento di un sistema carbonatico piattaforma-bacino nel Trias superiore della Catena Costiera calabrese, 117. Bollettino della Società Geologica Italiana, pp. 313–331.

Iovine, G., Guzzetti, F., Aceto, L., Antronico, L., Bruno, C., Caloiero, D., D'onofrio, F. Frustaci, Gabriele, S., Giordano, S., Greco, R., Gullà, G., Iaquinta, P., Petrucci, O., Santaloia, F., Soleri, S., Terranova, O., Valente, E., Chiesa, S., Galgaro, A., Lombardo, G., Muto, F., Rizzo, E., Manzella, A., 2012. The VIGOR Project–Evaluating the geothermal potential in the regions of "convergence". Activities and first results in Calabria. Rend. Online Soc. Geol. Ital. 21, 823–825.

Italiano, F., Bonfanti, P., Pizzino, L., Quattrocchi, F., 2010. Geochemistry of fluids discharged over the seismic area of the Southern Apennines (Calabria region, Southern Italy): implications for fluid-fault relationships. Appl. Geochem. 25, 540–554.

Jaupart, C., Mareschal, J.C., Schubert, G., 2007. Heat flow and thermal structure of the lithosphere. Treatise Geophys 6, 217–252.

Kumar, A., 2022. V2RhoT. Zenodo. https://doi.org/10.5281/ZENODO.6538257.

Lewicki, J.L., Bergfeld, D., Cardellini, C., Chiodini, G., Granieri, D., Varley, N., Werner, C., 2005. Comparative soil CO2 flux measurements and geostatistical estimation methods on Masaya volcano, Nicaragua. Bull. Volcanol. 68 (1), 76–90.

Maesano, F.E., Tiberti, M.M., Basili, R., 2017. The Calabrian Arc: three-dimensional modelling of the subduction interface. Sci. Rep. 7 (1), 8887.

Marini, L., Vespasiano, G., De Rosa, R., Viccaro, M., Principe, C., Bloise, A., Fuoco, I., Lelli, M., La Russa, M.F., Caruso, C.G., Gattuso, A., Lazzaro, G., Longo, M., Guido, A., Muto, F., Russo, L., Ciniglia, F., Tsegaye, A.A., Apollaro, C., 2025. The geothermal resources of Vulcano Island (Aeolian archipelago, Italy). Renew. Energy 253, 123622. https://doi.org/10.1016/j.renene.2025.123622.

Mattei, M., Cipollari, P., Cosentino, D., Argentieri, A., Rossetti, F., Speranza, F., Di Bella, L., 2002. The Miocene tectono-sedimentary evolution of the southern Tyrrhenian Sea: stratigraphy, structural and palaeomagnetic data from the on-shore Amantea basin (Calabrian Arc, Italy). Basin Res. 14 (2), 147–168. https://doi.org/10.1046/j.1365-2117.2002.00173.x.

Moeck, I.S., 2014. Catalog of geothermal play types based on geologic controls. Renew. Sustain. Energy Rev. 37, 867–882.

Montanari, D., Bonini, M., Corti, G., Agostini, A., Del Ventisette, C., 2017. Forced folding above shallow magma intrusions: Insights on supercritical fluid flow from analogue modelling. J. Volcanol. Geotherm. Res. 345, 67–80.

Moya, D., Aldás, C., Kaparaju, P., 2018. Geothermal energy: Power plant technology and direct heat applications. Renew. Sustain. Energy Rev. 94, 889–901.

Muto, F., Perri, E., 2002. Tectonic-sedimentary evolution of the Amantea basin, western Calabria (Evoluzione tettono-sedimentaria del bacino di Amantea, Calabria occidentale). Ital. J. Geosci. 121, 1–19.

Ortolano, G., Cirrincione, R., Pezzino, A., 2005. PT evolution of Alpine metamorphism in the southern Aspromonte Massif (Calabria - Italy). Schweiz. Mineral. Petrogr. Mitt. 85, 31–56.

Ortolano, G., Cirrincione, R., Pezzino, A., Puliatti, G., 2013. Geo-Petro-Structural study of the Palmi shear zone: Kinematic and rheological implications. Rend. Online Soc. Geol. Ital. 29, 126–129.

Ortolano, G., Cirrincione, R., Pezzino, A., Tripodi, V., Zappalà, L., 2015. Petro-structural geology of the Eastern Aspromonte Massif crystalline basement (southern Italy-Calabria): an example of interoperable geo-data management from thin section - to field scale. J. Maps 11 (1), 181–200.

Pepe, F., Sulli, A., Bertotti, G., Cella, F., 2010. Architecture and Neogene to Recent evolution of the western Calabrian continental margin: An upper plate perspective to the Ionian subduction system, central. Mediterr. Tecton. 29 (3).

Perrone, V., 1996. Une nouvelle hypothèse sur la position paléogéographique et l'èvolution tetonique des Unitès de Verbicaro et de San Donato (region Calabro-Lucanienne; Italie): implications sur le limite Alpes-Apennines en Calabre. C. R. Acad. Sci. Paris 322, 877–884.

Pezzino, A., Angi, G., Cirrincione, R., De Vuono, E., Fazio, E., Fiannacca, P., Lo Giudice, A., Ortolano, G., Punturo, R., 2008. Alpine metamorphism in the Aspromonte Massif: implications for a new framework for the southern sector of the CalabriaPeloritani Orogen (Italy). Int. Geol. Rev. 50, 423–441.

Pezzino, A., Pannucci, S., Puglisi, G., Atzori, P., Ioppolo, S., Lo Giudice, A., 1990. Geometry and metamorphic environment of the contact between the Aspromonte - Peloritani Unit (Upper Unit) and Madonna dei Polsi Unit (Lower Unit) in the central Aspromonte area (Calabria), 109. Bollettino della Società Geologica Italiana, pp. 455–469.

Piluso, E., Cirrincione, R., Morten, L., 2000. Ophiolites of the Calabrian peloritan arc and their relationships with the crystalline basement (Catena Costiera and Sila Piccola, Calabria, southern Italy) Glom 2000 excursion guide-book. Ofioliti 25 (2), 117–140.

Platt, J.P., Compagnoni, R., 1990. Alpine ductile deformation and metamorphism in a Calabrian basement nappe (Aspromonte, south Italy). Eclogae Geol. Helv. 83, 41–58.

Punturo, R., Kern, H., Cirrincione, R., Mazzoleni, P., Pezzino, A., 2005. P-and S-wave velocities and densities in silicate and calcite rocks from the Peloritani Mountains, Sicily (Italy): The effect of pressure, temperature and the direction of wave propagation. Tectonophysics 409 (1-4), 55–72.

Rossetti, F., Faccenna, C., Goffe, B., Monie, P., Argentieri, A., Funiciello, R., Mattei, M., 2001. Alpine structural and metamorphic segnature of the Sila Piccola Massif nappe stack (Calabria, Italy): insights for the tectonic evolution of the Calabrian Arc. Tectonics 20, 112–133.

Rybach, L., Mongillo, M., 2006. Geothermal sustainability-a review with identified research needs. GRC Trans. 30, 1083–1090.

Saito, H., McKenna, S.A., Zimmerman, D.A., Coburn, T.C., 2005. Geostatistical interpolation of object counts collected from multiple strip transects: Ordinary kriging versus finite domain kriging. Stoch. Environ. Res. Risk Assess. 19 (1), 71–85.

Santini, S., Basilici, M., Invernizzi, C., Jablonska, D., Mazzoli, S., Megna, A., Pierantoni, P.P., 2021. Controls of radiogenic heat and moho geometry on the thermal setting of the marche region (Central Italy): an analytical 3D geothermal model. Energies 14, 6511. https://doi.org/10.3390/en14206511.

Santini, S., Basilici, M., Invernizzi, C., Mazzoli, S., Megna, A., Pierantoni, P.P., Spina, V., Teloni, S., 2020. Thermal structure of the northern outer albanides and adjacent adriatic crustal sector, and implications for geothermal energy systems. Energies 13, 6028. https://doi.org/10.3390/en13226028.

Scandone, P., 1982. Structure and evolution of the Calabrian Arc. Earth Evol. Sci. 3, 172–180.

Scrocca, D., 2003. CROP Atlas: Seismic Reflection Profiles of the Italian Crust. Memorie Descrittive della Carta Geologica d'Italia, 62. Servizio Geologico d'Italia (APAT), Rome.

Sgroi, T., de Nardis, R., Lavecchia, G., 2012. Crustal structure and seismotectonics of central Sicily (southern Italy): new constraints from instrumental seismicity. Geophys. J. Int. 189 (3), 1237–1252.

Stacey, F.D., 2007. Mantle, Thermal Conductivity. In: Gubbins, D., Herrero-Bervera, E. (Eds.), Encyclopedia of Geomagnetism and Paleomagnetism. Springer, Dordrecht. https://doi.org/10.1007/978-1-4020-4423-6_213.

Tansi, C., Critelli, S., Folino Gallo, M., Gervasi, A., Imbrogno, G., La Rocca, M., Ponte, M., Tripodi, V., Muto, F., 2024. Seismotectonics and landslides of the NE border of the Calabrian Arc (Southern Italy). J. Maps 20 (1), 2347901. https://doi.org/10.1080/17445647.2024.2347901.

Tansi, C., Folino Gallo, M., Muto, F., Perrotta, P., Russo, L., Critelli, S., 2016. Seismotectonics and landslides of the Crati Graben (Calabrian Arc, Southern Italy). J. Maps 12 (sup1), 363–372. https://doi.org/10.1080/17445647.2016.1223760.

Tansi, C., Muto, F., Critelli, S., Iovine, G., 2007. Neogene-Quaternary strike-slip tectonics in the central Calabrian Arc (Southern Italy). J. Geodyn. 43 (3), 393–414. https://doi.org/10.1016/j. jog.2006.10.006.

Thierry, S., Dick, S., George, S., Benoit, L., Cyrille, P., 2019. EMODnet Bathymetry a compilation of bathymetric data in the European waters. In: OCEANS 2019-Marseille. IEEE, pp. 1–7.

Thomson, S.N., 1994. Fission track analysis of the crystalline basement rocks of the Calabrian Arc, southern Italy: evidence of Oligo-Miocene lateorogenic extension and erosion. Tectonophysics. 238, 331–335.

Tortorici, L., 1982. Lineamenti geologico-strutturali dell'Arco Calabro Peloritano. Rend. Soc. Ital. Mineral. Petrol. 4, 927–940.

Tortorici, L., Catalano, S., Monaco, C., 2009. Ophiolite-bearing mélanges in southern Italy. Geol. J. 44 (2), 153–166.

Tortorici, L., Monaco, C., Tansi, C., Cocina, O., 1995. Recent and active tectonics in the Calabrian Arc (Southern Italy). Tectonophysics 243, 37–55.

Tripodi, V., Gervasi, A., La Rocca, M., Muto, F., 2022. Seismotectonics of southern Calabria Terrane (south Italy). J. Mt. Sci. 19 (11), 3148–3162. https://doi.org/10.1007/s11629-022-7354-1.

Tripodi, V., Muto, F., Brutto, F., Perri, F., Critelli, S., 2018. Neogene-Quaternary evolution of the forearc and backarc regions between the Serre and Aspromonte Massifs, Calabria (southern Italy). Mar. Pet. Geol. 95, 328–343. https://doi.org/10.1016/j.marpetgeo.2018.03.028.

Trumpy, E., Manzella, A., 2017. Geothopica and the interactive analysis and visualization of the updated Italian National Geothermal Database. Int. j. Appl. Earth Obs. Geoinf. 54, 28–37.

Trumpy, E., Botteghi, S., Caiozzi, F., Donato, A., Gola, G., Montanari, D., Pluymaekers, M., Santilano, A., Van Wees, J., Manzella, A., 2016. Geothermal potential assessment for a low carbon strategy: a new systematic approach applied in southern Italy. Energy 103, 167–181. https://doi.org/10.1016/j.energy.2016.02.144.

Van Dijk, J.P., Bello, M., Brancaleoni, G.P., Cantarella, G., Costa, V., Frixa, A., Golfetto, F., Merlini, S., Riva, M., Torricelli, S., Toscano, C., Zerilli, A., 2000. A regional structural model for the northern sector of the Calabrian Arc (southern Italy). Tectonophysics 324, 267–320.

Vespasiano, G.*, Marini, L., Muto, F., Auque, L.F., De Rosa, R., Jimenez, J., Gimeno, M.J., Pizzino, L., Sciarra, A., Cianflone, G., Cipriani, M., Guido, A., Fuoco, I., Barca, D., Dotsika, E., Bloise, A., Apollaro, C., 2023. A multidisciplinary geochemical approach to geothermal resource exploration: the Spezzano Albanese thermal system, Southern Italy. Mar. Pet. Geol. 155. https://doi.org/10.1016/J.Marpetgeo.2023.106407. ISSN: 0264-8172.

Vespasiano, G., et al., 2014. Chemical and isotopic characteristics of the warm and cold waters of the Luigiane Spa near Guardia Piemontese (Calabria, Italy) in a complex faulted geological framework. Appl. Geochem. 41, 73–88. https://doi.org/10.1016/j.apgeochem.2013.11.014.

Vespasiano, G., Apollaro, C., De Rosa, R., Muto, F., Larosa, S., Fiebig, J., Mulch, A., Marini, L., 2015c. The Small Spring Method (SSM) for the definition of stable isotope - elevation relationships in Northern Calabria (Southern Italy). Appl. Geochem. 63, 333–346.

Vespasiano, G., Apollaro, C., Muto, F., De Rosa, R., Critelli, T., 2015a. Preliminary geochemical and geological characterization of the thermal site of Spezzano Albanese (Calabria, South Italy). Rend. Online Soc. Geol. It. 33, 108–110.

Vespasiano, G., Apollaro, C., Muto, F., De Rosa, R., Dotsika, E., Marini, L., 2015b. Preliminary geochemical characterization of the warm waters of the Grotta delle Ninfe near Cerchiara di Calabria (South Italy). Rend. Online Soc. Geol. It. 39, 130–133.

Vespasiano, G., Marini, L., Apollaro, C., De Rosa, R., 2016. Preliminary geochemical characterization of the thermal waters of Caronte SPA springs (Calabria, South Italy). Rend. Online Soc. Geol. It. 39, 138–141.

VIDEPI project. 2026, Visibilità Dati Esplorazione Petrolifera in Italia. https://www.videpi.com/videpi/videpi.asp.

VIGOR project. 2026, Evaluation of the geothermal potential of the convergence regions. http://www.vigor-geotermia.it/.

Vila, M., Fernandez, M., Jimenez-Munt, I., 2010. Radiogenic heat production variability of some common lithological groups and its significance to lithospheric thermal modeling. Tectonophysics 490, 152–164. https://doi.org/10.1016/j.tecto.2010.05.003.

Villamizar-Escalante, N., von Hagke, C., Muto, F., Caracciolo, L., Dremel, F., Friedrichs, B., Robl, J.,., Gallen, S., 2025. Slab length and slab tearing control asymmetric exhumation of the Calabrian Arc. Earth-Sci. Rev. 270, 105255. https://doi.org/10.1016/j.earscirev.2025.105255.

Waples, D.W., 2001. A new model for heat flow in extensional basins: radiogenic heat, asthenospheric heat, and the Mckenzie model. Nat. Resour. Res. 10, 227–238. https://doi.org/10.1023/A:1012521309181.

Webster, R., Oliver, M.A., 2007. Geostatistics for environmental scientists. John Wiley & Sons.

Zecchin, M., Civile, D., Caffau, M., Critelli, S., Muto, F., Mangano, G., Ceramicola, S., 2020. Sedimentary evolution of the neogene- quaternary crotone basin (Southern Italy) and relationships with large-scale tectonics: a sequence stratigraphic approach. Mar. Pet. Geol. 117, 104381.

Zhu, H., Bozdag, E., Tromp, J., 2015. Seismic structure of the European upper mantle based on adjoint tomography. Geophys. J. Int. 201, 18–52. https://doi.org/10.1093/gji/ggu492.